

AD624514

SYMMETRICAL LASER CRYSTALS

FINAL TECHNICAL REPORT

Period: 1 May 1963-31 October 1965

November 30, 1965

CLEARINGHOUSE
FOR FEDERAL AGENCIES AND
TECHNICAL INFORMATION

Harder

\$3.00	10.75	7.50	20
--------	-------	------	----

ARCHIVE COPY

Card 1

Contract Nonr-4131(00)
Program Code Number 3730
Authorization ARPA Order 306-62
Task Number NR017-708

SYMMETRICAL LASER CRYSTALS

FINAL TECHNICAL REPORT

Period: 1 May 1963-31 October 1965

November 30, 1965



Reproduction in whole or in part is permitted for any purpose of the United States Government.

This research is a part of Project DEFENDER under the joint sponsorship of the Advanced Research Projects Agency, the Office of Naval Research and the Department of Defense.

Union Carbide Corporation, Linde Division
Speedway Laboratories
P. O. Box 24184
Indianapolis, Indiana 46224

TABLE OF CONTENTS

List of Tables.	ii
List of Figures.	ii
FOREWORD	
SUMMARY.	I
INTRODUCTION.	II
DISCUSSION OF PEROVSKITE SYSTEMS AS SYMMETRIC HOSTS FOR DOPANT IONS	
A. Cubic Perovskites.	III - 1
B. Crystal Chemistry and Doping.	III - 2
C. Growth Methods.	III - 5
DEVELOPMENT OF THE SKULL-MELTING TECHNIQUE	
A. General Concept of Skull-Melting as Applied to Refractory Oxides	IV - 1
B. Inductive Coupling to Melts.	IV - 2
C. The Electrical Conductivity of Oxide Melts.	IV - 9
D. Design and Operating Problems in Skull-Melting.	IV - 11
EXPERIMENTAL RESULTS AND MATERIALS	
A. Analysis of Verneuil-Grown, Mn-doped SrTiO_3	V - 1
B. Summary of Skull-Melting Experiments.	V - 1
REFERENCES	
APPENDIX - THE ELECTRICAL CONDUCTIVITY OF LIQUID Al_2O_3 (MOLTEN CORUNDUM AND RUBY).	
	A

LIST OF TABLES

	Table
Complex Effective Permeability.	I
Summary of Skull-Melting Experiments.	II

LIST OF FIGURES

	Figures
Complex Effective Permeability, K^*	1
Complex Effective Permeability (Complex Plane).	2
Complex Plane Map.	3
Simple Coil and Load.	4
Skull-Melting Coil, Vessel and Load.	5
Electrical Conductivities of Various Substances as a Function of $1/T$ °K. .	6
Triangular Assembly for Skull-Melting.	7
Photographs of Skull-Melts of SrTiO_3	8

FOREWORD

This report constitutes the Final Report on work performed by the Crystals Research Group of the Speedway Laboratories under Contract Nonr 4131(00). The program has been directed by Dr. O. H. Nestor, the Principal Investigator, and monitored by Dr. Van O. Nicolai of the Physics Branch of the Office of Naval Research. All recent experimental work has been performed by Dr. H. Fay, Mr. C. D. Brandle and Mr. B. J. Corbitt. Previous contributors to the program include Dr. L. G. Tensmeyer, Mr. E. T. Fritsche, Mr. J. W. Lyle, Mr. R. G. Rudness, Mr. R. L. Hutcheson, Mr. A. M. Broyer, Mr. R. L. Brindle and Mr. G. W. Edwards. The electron-spin-resonance studies were made by Dr. Paul H. Kasai of the Union Carbide Research Institute. This Final Report was written by Dr. H. Fay. It reviews the entire program but specifically includes the period from January 1, 1965 to October 31, 1965.

I. SUMMARY

The development of cubic perovskites as symmetric hosts for laser dopant ions is of interest because long fluorescent lifetimes are to be expected. Other work on $\text{LaAlO}_3\text{:Cr}$ appears to confirm this. The simple II-IV perovskites are of interest as hosts for divalent and tetravalent dopants, but only four such compounds SrTiO_3 , SrSnO_3 , BaSnO_3 and BaZrO_3 are known to be cubic at room temperature. The low dielectric properties and stability toward reduction of BaZrO_3 makes it the most attractive potential host. The refractory nature of this compound has heretofore prohibited melt synthesis of single crystal BaZrO_3 .

A novel crucible-less melting technique, referred to as "skull-melting", has been studied intensively as a means for producing single crystals of BaZrO_3 (and also SrTiO_3). The process involves inductive coupling of electromagnetic radiation directly to the melt which acts as its own susceptor. The effects of many of the numerous variables, both thermal and electrical, on the process have been studied. The coupling of energy is found to depend primarily on the frequency and the size and electrical conductivity of the melt. Numerous experiments have demonstrated that SrTiO_3 (and BaTiO_3) may be fused by this process in a nearly reproducible manner and maintained in the molten state apparently indefinitely. Many attempts have been made to pull single crystals of SrTiO_3 (and BaTiO_3) but only dark, polycrystalline masses of partially deoxidized material have been obtained.

The fusion of large quantities of BaZrO_3 has also been accomplished by the skull-melting process. Melts have been sustained for several hours but it is uncertain whether or not a true "steady state" has been obtained. A loss of coupling frequently occurred and this is attributed to a gradual decrease in the electrical conductivity of the melt. When alumina was tested for comparison, a similar difficulty in sustaining the melts was encountered, nor did we succeed in pulling sapphire crystals from skull-melted alumina. The synthesis of single crystals of BaZrO_3 from the melt, a principal objective in the symmetrical laser host program, has not yet been accomplished, due to difficulties in the skull-melting process.

These experiments indicate that the electrical conductivities of molten oxides may be much lower than that given in the literature. The electrical conductivity of liquid Al_2O_3

has been directly measured with iridium electrodes at 2400°K and found to be 384 ± 5 mho/m. This is a factor of four lower than the accepted value but may still be higher than the "intrinsic" conductivity of the "pure" oxide.

The state of the manganese ions in Mn-doped SrTiO_3 , produced early in this program by the Verneuil method, has been investigated by electron-spin-resonance spectroscopy (ESR). Only divalent manganese, Mn^{+2} , was detected. This confirms previous suspicions that tetravalent manganese, Mn^{+4} , cannot be stabilized in the SrTiO_3 crystal.

II. INTRODUCTION

The overall objective of the program on symmetrical laser crystals is to obtain better crystal host-dopant combinations for giant pulse lasers. For this purpose it is desirable that the fluorescent lifetime of the dopant ions, as it exists in the host, be reasonably long. In many cases of interest (e. g. divalent rare earth ions) the transition is forbidden in the free atom. The ion in the crystal will, in general, behave differently and fluorescent lifetimes are usually quite short. If, however, the ion occupies a symmetrical site in the crystal, it is expected to be more nearly like the free atom. This contract is a part of a greater effort under ARPA Order 206-62, Program Code Number 3730, 4730, to establish the validity of this premise and to determine to what extent fluorescent lifetimes can be effected.

The lengthening of the fluorescent lifetime of an ion by placing it in a centrosymmetric site appears to be substantiated by work with LaAlO_3 crystals. The lifetime of Cr^{+3} has been reported to be $25^{(1)}$ to $34^{(2)}$ milliseconds in LaAlO_3 compared to 3 ms in ruby. The lifetime of Nd^{+3} appears to be increased by a factor of two (2) . This compound is nearly, but not exactly cubic. The Cr^{+3} enters the B-site which is centrosymmetric while the Nd^{+3} enters the A-site which is not quite centrosymmetric. (3) This may explain the difference in lifetime enhancement of Cr^{+3} vs Nd^{+3} .

The specific objective of this investigation is to grow cm^3 -sized crystals of cubic perovskites of the type $\text{A}^{+2}\text{B}^{+4}\text{O}_3$ activated with divalent or tetravalent cations. The aim is as above, to provide a centrosymmetric site for the dopant ion and thereby enhance its lifetime. A further objective is to have the dopant ion enter the crystal lattice by isoelectronic substitution for one of the host ions. The isoelectronic substitution creates no electronic defects in the crystal and removes the need for charge compensators. The II-IV perovskite oxides are of particular interest because there are certain divalent and tetravalent dopants that have desirable fluorescent characteristics. The divalent rare earth ions are of particular interest. (4)

Of the known perovskites, few appear attractive for this application. As discussed below and in the previous Semi-Annual Summary Report⁽⁵⁾, barium zirconate is still thought to be potentially the best "host" for substitutional doping with divalent rare earth ions. This compound is extremely refractory and the usual techniques of making oxide crystals are not applicable. Early experiments on flux growth of BaZrO_3 had led to the conclusion that a melt technique, or more particularly a Czochralski pulling method, would be more desirable, provided that a means of melting and containing this compound could be found. No crucible materials were known that could be used without attack at the required temperatures. The only way to contain a melt of BaZrO_3 appeared to be self-containment, in a "skull" of solid BaZrO_3 . Initial experiments had indicated that refractory oxides could indeed be melted in a skull of the same oxide, by direct coupling with a radio-frequency induction coil. These and later experiments also have shown that there are many difficulties to overcome before the method could be successfully applied to crystal growth by the Czochralski method. Many skull-melting experiments have been carried out under conditions that appeared to be nearly satisfactory for crystal growth, but failed because we either could not nucleate and pull single crystals from the melt, or because of slow physiochemical changes that occurred in the system which made it progressively more difficult to maintain the melt. The latter difficulty appeared to be most pronounced in systems, such as alumina, where it is well known that single crystals can be pulled from melts. The only apparent way to resolve these difficulties appeared to be by improved design of the skull-melting process in order to better match the characteristics of the system being melted. This in turn requires a fairly complete understanding of the skull-melting process. Much effort in this period has, therefore, been directed toward improved analysis of the skull-melting process, measurement of the electrical conductivity of alumina melts and a scaling-up of the melting apparatus for more efficient coupling to melts.

III. DISCUSSION OF PEROVSKITE SYSTEMS AS SYMMETRIC HOSTS FOR DOPANT IONS

A. Cubic Perovskites:

In order to fulfill the requirement that the dopant ion enter the lattice substitutionally in a site of high symmetry, the host perovskite should be cubic. The ideal perovskite structure (ABO_3) is cubic and has the symmetry of space group $Pm\bar{3}m$. Both the A-sites and the B-sites are centrosymmetric (symmetry element $\bar{1}$) and, therefore, either should be good sites for doping. However, most so-called perovskites are "derivative structures" or displacive distortions of the ideal perovskite structure. Furthermore, almost all perovskites exhibit one or more phase transitions over the temperature range from 0° K to their melting points. When phase transitions do occur, the lower temperature forms are of lower symmetry than the cubic space group $Pm\bar{3}m$. This, however, may or may not destroy the center of symmetry at the cation sites. In fact, the best example to date of fluorescent lifetime enhancement is that of Cr^{+3} -doped $LaAlO_3$, cited above. At room temperature this compound is rhombohedral-trigonal ($R\bar{3}m$) and only the Al^{+3} ions are truly at a center of symmetry.

Only the $A^{+2}B^{+4}O_3$ perovskites have been considered in this investigation. The problem of finding ideally cubic II-IV perovskites has been discussed at length in the previous report.⁽⁵⁾ While many well known II-IV perovskites, such as $BaTiO_3$, transform to the cubic as the temperature is increased, there are only four compounds that have been shown to be cubic at room temperature. They are $SrTiO_3$, $SrSnO_3$, $BaSnO_3$ and $BaZrO_3$. Of these four perovskites $SrTiO_3$ and $BaZrO_3$ were chosen for study in this investigation. Both of these compounds are apparently ideally cubic from their melting points down to cryogenic temperatures (110°K in the case of $SrTiO_3$). The ionic radii are also such that $BaZrO_3$ should offer a suitable site for doping with divalent rare earth ions Sm^{+2} , Eu^{+2} and Yb^{+2} . Of these ions Sm^{+2} is of the most interest for laser applications;⁽⁴⁾ the other ions are of interest because of their ease of reduction and stability in the divalent state. Similarly, the radii in $SrTiO_3$ should permit substitution of Mn^{+4} in the Ti^{+4} -site.

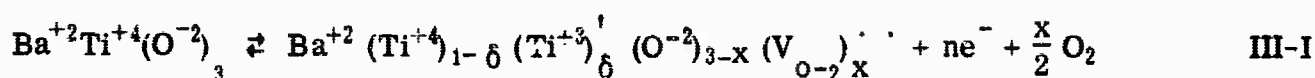
When working with II-IV perovskite compounds, one cannot completely avoid considering the phenomena of "ferroelectricity" and "antiferroelectricity" which are so

prominent in these compounds. The degradation of the cubic phase to phases of lower symmetry is often considered to be the result of electrical interactions, as for example in Devonshire's theory of BaTiO_3 .⁽⁶⁾ When ferroelectricity (or antiferroelectricity) occurs, the polarization, and presumably also the local fields in the crystal, can become very high. This situation is probably undesirable for lifetime enhancement of a dopant ion. Not only is the site non-centrosymmetric but the electrical effects of even a slight distortion may be very large. It is rather unlikely that "free ion" behavior will occur under these conditions. On this basis one should avoid ferroelectric and antiferroelectric perovskites. Even in the cubic or "paraelectric" state such compounds have large polarizabilities and unfavorable electrical effects should be anticipated. It is, therefore, noteworthy that none of the four cubic compounds above are known to be ferroelectric. SrTiO_3 does have a high dielectric constant which follow a Curie-Weiss law to low temperatures. A displacive transition is known to occur in the vicinity of 110°K, possibly to an antiferroelectric state, even though the departure from cubic symmetry is exceedingly small.⁽⁷⁾ The other compounds do not have notably high dielectric constants. For example BaZrO_3 ⁽⁸⁾ has a dielectric constant of about 40 at room temperature and this decreases only slightly with increasing temperature.

B. Crystal Chemistry and Doping:

The defect chemistry of II-IV perovskites was briefly considered in the previous report⁽⁵⁾. The work done since this has not altered the descriptions that have been given. Some further observations have been made on the tendency of the titanates (SrTiO_3 and BaTiO_3) to lose oxygen with a corresponding reduction of Ti^{+4} to Ti^{+3} . These compounds form melts which are appreciably conductive and which are relatively easy to maintain by the skull-melting technique. However, it is well known that it is extremely difficult if not impossible to "pull" single crystals of these substances from stoichiometric melts by the Czochralski technique. The most likely reason for this difficulty is that the intrinsic electronic defects create a high optical absorption, which grossly inhibits heat transfer in the crystal. High melting oxides which are opaque to radiation are not well suited to Czochralski growth and this appears to be the case with the titanates.

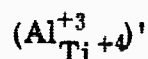
However, it should be possible to alter the conductivity and absorptivity by doping. We have, therefore, made a few doping experiments with skull-melted BaTiO_3 in order to see if we could not alter the material in such a way that we could pull single crystals. SrTiO_3 would presumably behave in a similar manner. BaTiO_3 was used merely because its lower melting point permitted easier operation and observation. These experiments are described more fully in section V-B below. Only the defect structure is considered here. The intrinsic defects in BaTiO_3 may be considered to be represented by the equations:



The crystal is thus assumed to be an oxygen deficient n-type semiconductor. However most of the oxygen deficiency is compensated for by the reduction of Ti^{+4} to Ti^{+3} . Now if the crystal is doped with lanthanum oxide, the La^{+3} will substitute for Ba^{+2} and create a "positive" lattice defect:



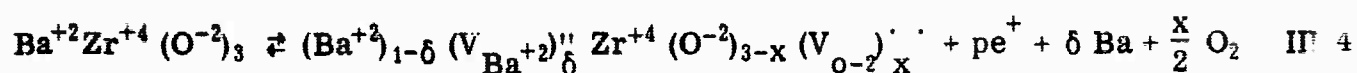
This will tend to increase the n-type conductivity (n), the reduction of titanium (δ), and decrease the oxygen vacancies (x). This behavior is well known, see for example Verwey.⁽⁹⁾ Our observations are in accord; La-doped BaTiO_3 is black, semiconducting and not at all conducive to Czochralski pulling. Doping with trivalent ions in the B-site should produce the opposite type of defect. When aluminum oxide is used to dope BaTiO_3 , the Al^{+3} produces a "negative" lattice defect



This will tend to decrease n and δ and increase the vacancies, x . When aluminum doping was tried the solidified melt was indeed lighter in color than "pure" BaTiO_3 . Although crystal pulling was still not successful, there was some indication of improvement. It

appears, therefore, that lattice defects, such as anion vacancies, are less deleterious to crystal growth by the Czochralski method than are electronic defects.

The situation in BaZrO_3 is quite different. There is no evidence of reduction of Zr^{+4} and, therefore, much less trouble with electronic defects. It has been stated⁽⁸⁾ that BaZrO_3 is a p-type semiconductor, with barium ion vacancies. However, the very high melting point of BaZrO_3 , coupled with the well known oxygen deficiency in other perovskite systems and in ZrO_2 , leads one to suspect the presence of oxygen vacancies also. One may postulate a structure such as:



where $2\delta = p + 2x$

Since BaO has such a large free energy of formation, it is most probable that any loss of Ba really corresponds to just a volatilization of the oxide with δ approximately equal to x and p very small. In any event, the compound is a much poorer electronic conductor than the titanates. As shown below, this lack of conductivity may be detrimental to the skull-melting process but it should be desirable for crystal growth.

In addition to the problems involved in growing II-IV perovskites as laser hosts, there are formidable problems in doping the host with divalent rare earth ions. The rare earths are normally trivalent and the divalent ions are strong reducing agents. Furthermore, in some cases the divalent ions may be unstable toward auto-oxidation-reduction or disproportionation according to the reaction:



If this reaction proceeds appreciably toward the right, then divalent doping will not be possible. However, the reaction is shifted toward the left by increasing temperature. Goldsmith and Pinch⁽¹⁰⁾ have estimated the temperatures below which the divalent rare earth ions are unstable. These "instability temperatures" are very high for lanthanum

and cerium and decrease to a minimum at europium. The instability temperature is again high for gadolinium and decreases to another minimum at ytterbium. Nd, Pm, Sm, Eu, Tm and Yb are estimated to be stable as divalent ions at room temperature. The others become stable at much higher temperatures. This stability will, of course, be influenced by the host. Goldsmith and Pinch⁽¹¹⁾ maintain that the divalent rare earths are less stable in oxides and sulfides than in halides. Thus, there is some question whether or not divalent rare earth ions can have a stable existence in the II-IV perovskite oxides. At the present we cannot prove or disprove this. In the present study we have only considered Sm^{+2} , Eu^{+2} and Yb^{+2} as likely to be stable. Even these ions would only be stable in a host that is very resistant toward reduction. SrTiO_3 is readily reduced and is therefore not satisfactory. BaZrO_3 is resistant toward reduction and may be satisfactory but this has still to be demonstrated.

C. Growth Methods:

A variety of growth methods have been investigated throughout the course of this study. In particular, samples of SrTiO_3 both undoped and doped with manganese, and of BaTiO_3 containing small additions of strontium, have been prepared by the Verneuil or flame fusion process. The growth of BaZrO_3 and SrZrO_3 from chloride-borate fluxes by the temperature decrease method, was also briefly studied. However, the ultimate use of perovskite crystals, in laser systems will demand material of both appreciable size and quality. Experience with other oxide crystals led us to conclude that a melt process would be most desirable in the long run, and further effort was directed toward melt-pulling processes or variations of the Czochralski method.

Based on theoretical considerations alone, BaZrO_3 is the best potential laser host material, of the simple II-IV perovskite compounds. The synthesis of sizeable single crystals of this compound has not previously been accomplished by any synthesis procedure. This substance is very refractory (mp > 2600°C) and the growth of this crystal is a very difficult problem. The flame-fusion method cannot be used to attain these temperatures, and there are no known crucible materials that are inert to attack by molten BaZrO_3 . In fact, there are no conventional methods of crystal growth that are applicable to the growth

of single crystal BaZrO_3 . The only way that we know of to contain a melt of stoichiometric BaZrO_3 , without reaction, is in a container or "skull" made of the compound itself. This process is referred to as "skull-melting" and has been used to advantage in certain metallurgical operations where contamination from crucibles must be avoided. Skull-melting differs from most fusion processes in that the thermal energy required to maintain the melt cannot be conducted through the container, since it is of the same composition, but must be supplied internally. This can be accomplished by radio-frequency induction heating, using the molten liquid as its own susceptor. The development of the skull-melting technique, as applied to BaZrO_3 and other oxides, is discussed in detail in the next section.

IV. DEVELOPMENT OF THE SKULL-MELTING TECHNIQUE:

A. General Concept of Skull-Melting as Applied to Refractory Oxides:

As mentioned above, "skull-melting" refers to the containment of a liquid "melt" in a solid "skull" of the same composition (or a composition in equilibrium with the melt). Furthermore, we apply this term here to describe a process wherein the liquid is used as its own susceptor for coupling of electromagnetic radiation from a radio-frequency power oscillator. This process is quite different from most other heating techniques and presents many novel problems. The systems of interest are oxides that are low loss dielectrics when solid and cold. These solids do not heat appreciably in electromagnetic fields, and it is therefore impossible to start a melt with the oxide alone. The initial melting must be accomplished by another external source of heat or by adding some conductive object to the charge. We have used the latter method almost exclusively, a solid conductive ring acting as the initial susceptor. After the melt is formed, the liquid itself should act as susceptor. The initial susceptor ring is now superfluous and should be removed or reacted in such a way that it does not contaminate the melt. The melt differs from the initial susceptor in that it is not rigid. The liquid-solid boundary is variable and will only be stationary when and if a "steady-state" is achieved. The attainment of such a steady state depends on the thermal and electrical properties of the melt itself, convective flow in the melt, radiation from the melt surface, heat transport by conduction and radiation through the skull wall and the geometry and electrical characteristics of the electrical driving network. Finally, these conditions must be alterable in a controlled manner so that the temperature at the center of the melt surface can be made correct for nucleation and growth of a single crystal by the Czochralski method.

Most of these problems were discussed in some detail in the previous report.⁽⁵⁾ There we showed how inductive coupling could be treated in terms of the "complex effective permeability" of the load, and how the engineering data developed for Eddy Current Testing by Förster^(12, 13) could be used to advantage. The problem of skull-boundary stability was approximately analyzed and it was shown that the skull should be stable provided that the melt radius is not too small. Experience has shown, however, that the melt and skull must be confined by some sort of container. The container must be made from material that is

a good thermal conductor, but yet it must not "short-out" the coupling to the melt. The simultaneous requirements of confinement and of close coupling of the power are in conflict and solutions must represent a compromise.

In Section B below, we extend the previous analysis of inductive coupling to include the "container" and show how it may be used to improve the coupling. In Section C the problem of the electrical conductivity of molten oxides is reviewed. Much of the difficulty in skull-melting is thought to be due to variations in the melt conductivity. Previous conclusions about melt conductivities are now in question. In Section D, the practical problems of skull-melting such as starting methods, container design and melt control are discussed.

B. Inductive Coupling to Melts:

Here we consider the problem of inductive coupling to melts (or any other load) which may be described by a complex effective permeability. First the problem of a simple single coil and load will be treated to obtain results similar to Förster's. The analysis will then be extended to circuits involving "containers" and "transformer" coupling. The analysis will show the advantages of using "idlers" or "link transformers" in skull-melting. The behavior of experimental equipment may be described in a semi-quantitative manner according to this analysis.

The load is assumed to be cylindrical of radius r_4 and to have a "complex effective permeability", $\mu^* = \mu_0 K^* = \mu_0 (K' - jK'')$. For nonmagnetic materials the values of K' and K'' must lie between 0 and 1, and will depend on the electrical conductivity, σ , and radius, r_4 , or diameter, d , of the object and on the frequency f . These variables may be combined to a single variable, F , where

$$F = \frac{\sigma d^2 f}{5.066 \times 10^5} \quad \text{IV - 1}$$

Förster has tabulated the values of K' and K'' for full cylinders⁽¹⁴⁾ in terms of F , the values are shown in Table 1 and graphically in Figures 1 and 2. Note that K' decreases monotonically with increasing F but that K'' goes from 0 to a maximum of .3775 at

$F = 6.25$ and then decreases again toward zero. The quantity K''/K' is also plotted in Figure 1. This is equivalent to $1/Q$ for the circuit and shows that Q is always greater than 1 but approaches 1 for high values of F .

To see how the complex effective permeability may be applied to the determination of circuit behavior, consider the simple circuit shown in Figure 4. The load is drawn below the diagram and identifies the primary current and voltage, the object radius, r_4 , the effective primary radius, r_1 and the effective permeabilities, K' and K'' . In this analysis and in those following, the "current-sheet equivalent" is used in calculating the inductance of the coil. Actual short helical coils will require corrections when the inductance is calculated from the dimensions but the current sheet equivalent radius may be found and employed for r_1 in lieu of the actual radius. We now analyze the equivalent circuit to determine the impedance as seen from the coil leads.

The "current-sheet" inductance is simply:

$$L_1 = \mu n^2 \times \frac{A_1}{\ell}$$

where μ is the permeability

A is the effective cross-section of the circuit IV - 2

ℓ is the length

n is the number of turns

The permeability is composed of two parts, that of the object and that of the free space between the object and coil. We may apportion this according to the relative areas.

Treating the object permeability as $\mu_o K^*$, we may write for μ :

$$\mu = \mu_o \left[1 - \left(\frac{r_4}{r_1} \right)^2 \cdot (1 - K^*) \right] \quad \text{IV - 3}$$

The square of the radius ratio is called the "filling factor", η_{14} . The inductance thus becomes:

$$L_1 = \frac{\mu_0 n^2 \pi r_1^2}{l} \left[1 - \eta_{14} (1 - K^*) \right] \quad \text{IV - 4}$$

If the object were absent, the second term would vanish and the inductance would be that of an empty coil, L_{10} . After expanding K^* , equation 4 becomes:

$$L_1^* = L_{10} \left[1 - \eta_{14} (1 - K') - j \eta_{14} K'' \right] \quad \text{IV - 5}$$

The inductance is thus complex. It is perhaps better to use the impedance $Z = j\omega L_1^* = R + j\omega L$ where:

$$\frac{\omega L}{\omega L_0} = \left[1 - \eta_{14} (1 - K') \right] \quad \text{IV - 6a}$$

$$\frac{R}{\omega L_0} = \eta_{14} K'' \quad \text{IV - 6b}$$

Equations (6) are identical with expression derived by Förster⁽¹⁵⁾ for eddy current testing. The relative resistance and reactance may be obtained directly from a graph of $\eta_{14} (1 - K')$ vs. $\eta_{14} K''$. Such a graph, which we call a complex plane map, is shown in Figure 3. The effect of the load is always to decrease the inductance by $\omega L_0 \eta_{14} (1 - K')$ and increase the resistance by $\omega L_0 \eta_{14} K''$. The graph also illustrates the importance of the filling factor, η_{14} ; heavy loading of the circuit requires a large value of η_{14} .

The analysis of the circuit is now complete. The primary voltage and current are related by:

$$e_1 = Zi_1 \quad \text{IV - 7}$$

The behavior of the entire circuit is thus described by an equivalent circuit of impedance Z .

Skull-melting experiments demand a circuit more complicated than that of Figure 4. Auxiliary structures are required to contain the melt. These structures are located between the coil and load and thus preclude having very high filling factors, η . If dielectric materials were used, the analysis would be similar to that above. In all practical cases, however, the "container" is made of water-cooled copper. Since the copper is a conductor, we must consider its effect on the circuit.

An advantageous geometry for skull-melting is shown in Figure 5. The container consists of three copper "leaves", separated so that they are electrically independent. The equivalent circuit defines the voltages, currents and radii in the following analysis. The thickness of the gap (the equivalent of all three gaps) is taken to be small and is neglected. This is a 3-loop circuit and the circuit equations may be written as: (impedance, Z , defined later)

$$\begin{aligned} e_1 &= Z_1 i_1 + Z_{12} i_2 + Z_{13} i_3 \\ e_2 &= Z_{12} i_1 + Z_2 i_2 + Z_{23} i_3 \\ e_3 &= Z_{13} i_1 + Z_{23} i_2 + Z_3 i_3 \end{aligned} \quad \text{IV - 8}$$

There are two additional conditions, namely; $e_2 = e_3$ and $i_2 = -i_3$. Equation (8) now becomes:

$$\begin{aligned} e_1 &= Z_1 i_1 - (Z_{12} - Z_{13}) i_3 \\ 0 &= (Z_{12} - Z_{13}) i_1 - (Z_2 + Z_3 - 2Z_{23}) i_3 \end{aligned} \quad \text{IV - 9}$$

Solving equations (9), we obtain the following relations:

$$i_1 = \frac{-(Z_2 + Z_3 - 2Z_{23}) e_1}{(Z_{12} - Z_{13})^2 - Z_1 (Z_2 + Z_3 - 2Z_{23})} \quad \text{IV - 10a}$$

$$i_3 = \frac{-(Z_{12} - Z_{13}) e_1}{(Z_{12} - Z_{13})^2 - Z_1 (Z_2 + Z_3 - 2Z_{23})} \quad \text{IV - 10b}$$

$$\frac{i_3}{i_1} = \frac{Z_{12} - Z_{13}}{Z_2 + Z_3 - 2Z_{23}} \quad \text{IV - 10c}$$

$$Z = \frac{e_1}{i_1} = Z_1 - \frac{(Z_{12} - Z_{13})^2}{Z_2 + Z_3 - 2Z_{23}} \quad \text{IV - 10d}$$

The impedances may now be defined as follows:

$$\begin{aligned} Z_1 &= j\omega L_1 & Z_{12} &= j\omega M_{12} \\ Z_2 &= j\omega L_2 & Z_{13} &= j\omega M_{13} \\ Z_3 &= j\omega L_3 & Z_{23} &= j\omega M_{23} \end{aligned} \quad \text{IV - 11}$$

The resistances of the metallic parts have been neglected. The inductances, however, are complex and may be written as:

$$\begin{aligned} L_1 &= \frac{\mu_0 n^2 \pi r_1^2}{\ell} \left[1 - \eta_{14} (1 - K^*) \right] = L_{10} \left[1 - \eta_{14} (1 - K^*) \right] \\ L_2 &= \frac{\mu_0 \pi r_2^2}{\ell} \cdot \left[1 - \eta_{24} (1 - K^*) \right] = L_{20} \left[1 - \eta_{24} (1 - K^*) \right] \\ L_3 &= \frac{\mu_0 \pi r_3^2}{\ell} \cdot \left[1 - \eta_{34} (1 - K^*) \right] = L_{30} \left[1 - \eta_{34} (1 - K^*) \right] \end{aligned} \quad \text{IV - 12}$$

The mutual inductances become:

$$\begin{aligned} M_{12} &= \frac{\mu_0 \pi n r_2^2}{\ell} \left[1 - \eta_{24} (1 - K^*) \right] \\ M_{13} &= \frac{\mu_0 \pi n r_3^2}{\ell} \left[1 - \eta_{34} (1 - K^*) \right] \\ M_{23} &= \frac{\mu_0 \pi r_3^2}{\ell} \left[1 - \eta_{34} (1 - K^*) \right] \end{aligned} \quad \text{IV - 13}$$

We may now substitute these quantities into equations (10c and 10d) to obtain:

$$\frac{i_3}{i_1} = n$$

$$\text{and } Z = j\omega \left[L_1 - n (M_{12} - M_{13}) \right] \quad \text{IV - 14}$$

$$= j\omega L_{10} \left[1 - \frac{r_2^2 - r_3^2}{r_1^2} - \eta_{14} (1 - K^*) \right] \quad \text{IV - 15}$$

Finally, we solve for the relative resistance and reactance as in equation (6) and obtain:

$$\frac{\omega L}{\omega L_0} = 1 - \frac{r_2^2 - r_3^2}{r_1^2} - \eta_{14} (1 - K') \quad \text{IV - 16}$$

$$\frac{R}{\omega L_0} = \eta_{14} K''$$

The analysis is now complete. The significance of the results, as they apply to skull-melting, may now be discussed. First we find from equation (14) that according to the "current sheet" approximation, the surface current in the metallic parts is simply the primary current times the number of turns. This simple relation is just the current transformer equation and applies even though the load is complex. Of more significance is the comparison of equations (6) and (16). The resistive part of the impedance is seen to be identical. Ideally, the container parts do not influence the loss. The presence of the filling factor, η_{14} , appears to make R dependent on the coil size. However, if we substitute for L_{10} in equation (16b) we obtain:

$$R = \frac{\omega \mu_0 n^2 \pi r_4^2}{l} K'' \quad \text{IV - 17}$$

and thus R depends only on the radius of the melt r_4 .

The inductance is affected by the presence of the container parts. They decrease the inductance in proportion to their cross sectional area in addition to the decrease produced by the load as given in equation (6). We may define an inductance, L_{11} , which is that of the assembly without the load. This inductance is given by

$$L_{11} = L_{10} \left[1 - \frac{r_2^2 + r_3^2}{r_1^2} \right] \quad \text{IV - 18}$$

The decrease in inductance caused by the container is beneficial; L_{11} should be as small as possible.

The reasons why a container design such as that of Figure 5 is desirable for skull-melting may be summarized as follows.

- (1) The conductivity, σ , of oxide melts is less than that of metals. Good coupling only occurs when k is in the range shown in Figure 1. This, in turn, requires that $f d^2$ be above a minimum value. However, d cannot be so large that radiation losses demand extremely large powers. Thus, the frequency, f , must be large.
- (2) A large value of f or ω requires that the coil inductance be small, if the coil is going to permit the flow of a large current. However, the coil must be large enough to accommodate the melt and container. This usually demands that L_{10} be fairly large.
- (3) The container parts, when arranged as in Figure 5 act to fill the "empty space" between coil and load and decrease the effective inductance so that a large primary current may flow. The resistance is not effected and the primary current generates power according to:

$$P = I_1^2 \omega L_{10} \eta_{14} K'' \quad \text{IV - 19}$$

It appears that with further practical experience, it might be possible to optimize the design of skull-melting equipment. So far this has not been attempted except to the extent indicated above.

Finally, it should be noted that all the equations developed here are for the same length, l . In fact, the relations are really true only for very long cylinders. When l is small and when the load length, ie. l_4 , is smaller than that of the container as is often the case, the analysis is much more difficult. In fact, there is no simple way of accounting for differences in lengths, without going back to the fields involved. It is thought that this problem is best approached empirically, by extending the concept of the "area-filling factor" to that of a "volume-filling factor". In this way we may use all the above equations by merely substituting for η_{14} the appropriate value of the volume filling factor. This value of η_{14} will be that which gives the same results as an infinite cylinder with an area ratio of η_{14} .

The application of these principles to actual experimental equipment is discussed in Section D below.

C. The Electrical Conductivity of Oxide Melts:

From the preceding analysis we find that efficient power delivery to the load will only occur when the parameter, F , is in the proper range. This, in turn, depends on the conductivity, σ , of the melt. When the conductivity is either too low or too high, the system will appear to be nearly a pure reactance and the power dissipation will be small. However, as shown by Figures 1, 2, and 3, the power dissipation should be appreciable for conductivity values which are about a factor of ten either side of the optimum. There have been very few measurements made to determine the conductivity of molten oxides. Van Arkel et al. ⁽¹⁶⁾ review the subject and report measurements on eight oxides (LiO , Bi_2O_3 , TeO_2 , PbO , MoO_3 , V_2O_5 , CrO_3 , and Sb_2O_3). Some additional "electric furnace" estimates are given for refractory oxides (MgO , CaO , TiO_2 , ZrO_2 , ThO_2 , Cr_2O_3 and Al_2O_3). The conductivities vary with temperature approximately according to an equation of the usual type;

$$\log \sigma = A + \frac{B}{T} \quad \text{IV-20}$$

from which activation energies may be calculated. Some of Van Arkel's results are shown

in Figure 6 along with other data on various metals, semi-conductors, salts, aqueous solutions, etc. for purposes of comparison. It appears that the molten oxides of interest should have conductivities of the order of 10^3 to 10^4 mho m^{-1} . They should then be better conductors than molten NaCl and the strongest of aqueous solutions, but poorer conductors than carbon and the metals.

The conductivity is related to the frequency, f , and the diameter of the coil, D , by the approximate equation:

$$2 f \text{ (mc)} = \frac{F}{\eta} \left(\frac{1}{\sigma D^2} \right) \quad \text{IV - 21}$$

Using this equation, we have calculated the optimum conductivity for a particular experimental arrangement ($f = 3$ mc, $\eta D^2 = 40 \times 10^{-4} m^2$, $F = 6.25$) to obtain a value of ca 260 mho/m, or $\log \sigma = 2.4$. This value lies below the values for oxides shown in Figure 6. We should, therefore, expect good coupling with these oxide melts. In fact, it appears as though the conductivities are somewhat higher than optimum. However, our experiments have shown that melts of the titanates, $BaTiO_3$ or $SrTiO_3$, may be readily maintained in this apparatus, but that melts of $BaZrO_3$ or Al_2O_3 behave as though their electrical conductivities were too low for efficient coupling. This has prompted us to seriously question the conductivity data for refractory oxides. It seemed from our observation that the conductivities given in Figure 6 might be far too high. Since the measurements on high melting oxides are all merely estimates from electric furnace operating characteristics, using carbon electrodes in the melt, it was thought that much of the reported conductivity could have come from contamination and was not "intrinsic". Direct measurements of the conductivities of these pure oxides are needed. In particular, we require the value for $BaZrO_3$. We have been unable to devise a method for directly measuring the conductivity of $BaZrO_3$, but we have developed a procedure applicable to melts of corundum, Al_2O_3 . This procedure and the results for Al_2O_3 are described fully in Appendix I. This experiment has been written as a separate paper and has been submitted for publication in the Journal of Physical Chemistry.

The measured conductivity of liquid Al_2O_3 was found to be 384 mho/m. This value is indeed lower by a factor of 4 than that reported by Van Arkel.⁽¹⁶⁾ However, this conductivity is still sufficient to make the melt a very good susceptor in our apparatus. The conductivity measurement did not, therefore, resolve the problem. As stated in the Appendix, the measurements were made under conditions which were somewhat reducing. It is quite possible that the conductivity in an oxidizing environment is still much lower. The other source of error could be the use of the simple semi-infinite cylinder formula for the calculations (e. g., equation IV-21). Corrections should be made because of the shortness of the melt. The "volume filling factor" mentioned above may be much less than we have estimated. In any event, however, these oxides behave in our apparatus as though they are much poorer conductors than they are supposed to be. The only way to improve the situation is to either increase the frequency or the size of the system or both. Therefore, we have attempted to scale up the system as described in the following section.

D. Design and Operating Problems in Skull-Melting

The first application of direct coupling of radio-frequency energy to oxide melts was the melting of manganese ferrite by Montefort et al.⁽¹⁷⁾ A special coil was made of "square" tubing. The spaces between the turns were sealed with an alumina-based cement. A special water cooled copper bottom was also used. The water circulating in the coil kept the assembly cool and thus protected against attack by the molten ferrite.

The initial experiments on perovskites were made by merely packing a coil with the powdered oxides. This simple approach has been applied to the fusion of several oxides, including SrTiO_3 , BaZrO_3 and ZrO_2 . However, there are disadvantages to this method. After liquid is formed, the melt will tend to increase in diameter until a steady state condition can develop at the skull wall. When the coil itself serves as the container and heat sink, the melt may tend to run out between the turns of the coil. The melt is a conductor and may also "short-out" part of the coil, creating arcs which can destroy the apparatus. Increasing the coil spacing makes it more difficult to contain the liquid, while decreasing the spacing may make arcing more likely. Similar problems are encountered in all designs. However, the "gap" problem is particularly severe with the simple packed

coil since the length of the gap is long and breakdown may occur at many places. The obvious cure for this problem is to confine the charge in some inert container (inert also in that it does not effect the electromagnetic field). Unfortunately, such a material is not known. Because the thermal power to the container may be quite large, it must be constructed of a good thermal conductor, such as copper, and well cooled by flowing water. Since the copper is a good electrical conductor, the container cannot completely enclose the melt without destroying the field inside. The confinement problem and the electrical problem are in direct conflict. All of the designs tested were thus attempts to find the appropriate compromise.

Several auxiliary container designs have been tested during this program. The first was a simple copper tube having a single longitudinal split of about 1/8-inch. Tubing was soldered to the outside for water cooling. Warping was a problem with this container; the gap would tend to spread during a run. A thicker walled container was then built. Cooling channels were milled in the copper and closed by means of an outer tube soldered on with silver solder. This was much better but both leaking of fluid and arcing were not uncommon. With SrTiO_3 , which tends to be a semiconductive solid, arcing was severe. Although the "split tube" type of container does not destroy the internal electromagnetic field, it does interact in two ways. The "skin depth" for copper is very small and surface currents are established in the container. As long as these currents do not enclose the melt, they do little harm. There is some detuning of the coil and some Joule heating in the copper, but these perturbations are not too bothersome. The container also behaves as an open-circuited one-turn coil and thus a voltage develops across the gap. When the voltage gets high and the gap small, the electric field may become high enough for "breakdown". Finally, there is some displacement current across the gap because of the distributed capacity. This current also encircles the melt, shielding it and is therefore detrimental. This effect is thought to be small. If arcing does occur, however, this short-circuit current will badly shield the melt.

These cylindrical containers were set up vertically inside the induction coil. One simple way to prevent the fluid melt from leaking out the gap is to turn the

coil and cylinder to a horizontal position with the gap on the top. There is then no need for the gap to be small; it can be opened to several inches and arcing across the gap will also be prevented. Several varieties of horizontal cylinders or "boats" have been built and tested. The simplest was similar to the thicker cylinder described above, but with a gap of ca. 2.5-inches. The cross-section resembled a letter "C". Another simple "boat" was made by bending a flat copper plate into a round-bottom "V". Cooling pipes were soldered on the external surface. These horizontal containers were found to be workable and several fusions of SrTiO_3 and BaZrO_3 have been made in them. Problems of a different nature are encountered with the horizontal boats. While there is no longer a problem of the liquid running out the gap, it must still be prevented from running out the ends. The solution to this problem appears to be to just make the vessel sufficiently long, relative to the coil, so that the melt eventually freezes as it grows longitudinally. Probing of the magnetic field along the axis of the coil showed that the field "fell off" rather quickly as the end of the coil was passed, in accord with elementary theory. When the boat is in place, however, the field is "stretched" and does not fall off so rapidly. Convective mixing of the melt also tends to transport fluid toward the ends. On numerous occasions the melt would tend to impinge on the ceramic "end-plugs". This condition is bothersome but could no doubt be cured by making the assembly sufficiently long. Still another boat was constructed by cutting two saw cuts perpendicular to the axis and half way through a large copper tube. The central section was then pressed or dented to form a reversed or reentrant cylindrical section, making the total cross section resemble a squat hollow "U". Flat bulkheads were then soldered on at the saw cut and at the ends. Finally, entrance and exit tubes are connected so that water can be passed through the hollow space in this "hollow-log" boat. The "hollow-log" boat has the advantage of rather easy fabrication, plus the end closures which prevent the melt from spreading longitudinally. The end sections do not apparently prevent the field from penetrating the melt in the central section. Unfortunately, the particular boat built was not sized properly for good coupling and although it appears satisfactory, it has not been tested in melting oxides. As experience was gained with the horizontal boats, their shortcomings were also brought out. If the skull is thin, arcing to the melt can occur at the top surface of the liquid. The current then flows through the copper and across the

top of the melt to complete the circuit. The top surface is well heated by both the arcs and the surface current, but the lower regions of the melt are shielded. The arcing need not be violent, but it erodes the vessel and introduces copper contamination into the melt. The arcs pass through the gas space between boat and liquid, rather than through the solid skull, and there is no simple way to stop them. Still another problem is the coil which must now pass over the top of the melt. Pulling of crystals is not prevented by the coil; the coil may be stretched sufficiently to allow passage of pull-rod and crystal. What is bothersome is the tendency for low ionization gases from the melt to contact the coil and initiate arcs. Various covers and shields have been used to protect the coil but there are no materials satisfactory for use with BaZrO_3 and the problem remains.

All of the horizontal melting systems are rather severe distortions of the circular cylindrical symmetry. A large quantity of melt must be created to fill up the vessel to a point where good coupling can occur. Experiments with vertical containers also continued and at this stage in the experimentation a vessel was made that appeared to be superior to its predecessors. This was achieved by increasing the number of gaps. Adding gaps may seem like a regression toward the original packed coil, but now the gaps were put in series. The optimum number of gaps is not known; in these experiments three gaps have been used. With three gaps a container can be constructed from the flat plates arranged in an equilateral triangle. This type of assembly is shown in Figure 7. The advantage of the multiple gap design is the lesser tendency to arcing. The gaps may be narrow enough to quench out the melt by the "thermal pinch" presented at the gap, but still not initiate arcs. This is undoubtedly because more than one gap must be jumped simultaneously in order to complete the circuit. The statistical chances for failure are reduced. This does not mean that arcing and electrical breakdown have not occurred at all, but only that the chances of successful operation are improved. The three gap design has been the most satisfactory of those tested.

The analysis given in Section B has shown the importance of close coupling and how to achieve this with proper design of the container. The triangular container is simple to fabricate, but difficult to hold together. Also, the coupling is not tight since there are large open regions. A more efficient design is that shown schematically in Figure 5. This

type of container has been used in all recent tests. One container had a 2.5-inch inside diameter, which at the time it was made, was thought to be as large as would be desirable for fusing BaZrO_3 since the radiation losses increase as the top surface area. This arrangement has been very satisfactory for fusing the titanates but, as shown above, it has been found to be very difficult to maintain melts of BaZrO_3 or even Al_2O_3 in this system. The fusions can be made, but as time progresses, ever increasing driving currents are required to maintain the melt. When the oscillator reaches full output the melt will become quiescent and freeze.

Recently, we have found a reference to earlier work by Sterling and Warren on melting of metals and semi-conductors without a crucible. ⁽¹⁶⁾ This process is quite similar to what we have termed skull-melting, except for the important difference that these workers were dealing only with good conductors. Sterling and Warren have used both horizontal and vertical container geometries and also what they have called a "cage crucible". The latter is made of silver tubing and looks something like an inverted bird cage. This design was apparently very satisfactory for pulling silicon crystals.

The problems described above indicated the necessity for us to scale up our equipment so as to be able to maintain melts of "apparently" low conductivity. An increase in frequency would also be advantageous, but this is difficult to achieve since we were already operating at nearly as high a frequency as we could with this type of coil. We have, in the past period, constructed a coil-container assembly similar to that shown in Figure 5, but with an internal diameter of five-inches. This container, however, differed from earlier designs, since it was necked-in at the bottom as in the cage crucible to help contain the liquid and prevent it from melting downward.

Several experimental runs have been made with the new container. The results were not very satisfactory. Fusions of Al_2O_3 have been made but the coupling was obviously not good and the melt could not be maintained. Furthermore, this assembly is a very complex load, electrically. There is considerable capacitance and several self-resonances in the frequency range where operation is possible. We believe now that much of the trouble is due to the incorporation of the "bottom" in this design and that this should be

removed. A similar problem did not apparently occur in the experiments of Sterling and Warren, possibly because they were working with metals whose conductivity is much greater than that of oxides. It is unfortunate that this latest container did little to resolve the container-coupling problem. Even after extensive experimentation, it is still uncertain whether or not oxides such as Al_2O_3 and BaZrO_3 lose coupling because of a gross decrease in conductivity of the melt, or merely because the container and driving coil are not properly designed for efficient coupling. The latter deficiency could be corrected by proper design but not the former.

A related problem is that of starting the melt. In the experiments of Monteforte et al.⁽¹⁷⁾ slugs of the metals whose oxides were to be fused were placed in the charge as initial susceptors. They also mention starting the melt with an oxy-hydrogen torch. In the work at Linde, several start-up procedures have been tried. Auxiliary heat sources have been found to be rather unsatisfactory for refractory substances. The auxiliary source must produce a temperature high enough to melt the oxides. This is very difficult for BaZrO_3 . Even if a heat source is available, it is usually only possible to heat the charge from the top. The heat will not penetrate the charge very well and only melts of shallow depth will be produced. Although not treated explicitly in the discussion of skull-melting, it has been found that a certain depth or thickness of the melt is required before effective coupling takes place. Auxiliary heat sources were therefore abandoned.

Two methods of starting have been mainly used, both involving the use of ring-shaped susceptors placed inside the charge of powdered oxides. In one method metal rings are used and in the other carbon rings. The metals chosen were always those corresponding to the tetravalent cation in the oxide system, thus titanium and zirconium. In this manner no contamination is introduced other than an eventual excess of oxide BO_2 , and this can be corrected if necessary. This is a most desirable procedure if the metal has a high enough melting point. For example, titanium metal rings may be used to initiate melts of SrTiO_3 (or other composition in the $\text{SrO} - \text{TiO}_2$ system near SrTiO_3). Titanium metal melts at 1670°C , which is well below the melting point of SrTiO_3 but higher than the $\text{SrTiO}_3 - \text{TiO}_2$ eutectic composition. The ring is buried in the powdered charge and heated mildly by inductive coupling to warm up the surroundings. After sintering occurs at ca. $1200\text{--}1400^\circ\text{C}$ more

power is admitted until the ring melts. An arc may establish when the ring melts or parts somewhere along its periphery. The arc is usually not detrimental but acts to add energy to the system. Under favorable circumstances, sufficient oxide melt will be formed to couple directly. After a period of build-up of the liquid puddle, the skull will form and stabilize. A similar procedure is used with zirconium rings to start melts of BaZrO_3 . Zirconium metal melts at 1857°C , but this is considerably less than the melting point of BaZrO_3 and even less than the $\text{BaZrO}_3 - \text{ZrO}_2$ eutectic temperature. Thus the molten metal must remain intact and act as a susceptor while the energy to fuse the oxides is built up. This has been accomplished, but it is difficult and uncertain. Furthermore, zirconium metal rings of appropriate size are difficult to obtain.

When carbon rings are used the situation is somewhat different. The carbon rings will not melt and it is much easier to control the warm-up period and the fusion. Once again, the ring may eventually part and initiate an arc but without detriment. Provision has been made for blanketing the experiment with oxygen gas, so that the carbon may be oxidized out of the melt. Complete removal of the carbon is easily achieved. The carbon-ring start-up procedure is easier to carry out than the metal-ring procedure and is the preferred method.

When either carbon or metal rings are employed, there is inevitably some local reduction of the melt. The reduction processes have not been investigated in any detail but the carbon and metals will behave differently in this respect. With titanium metal rings, Ti^{2+} , Ti^{3+} etc. may be formed in the charge and there is the likelihood of a number of complex intermediate compounds. With zirconium on the other hand, an equilibrium between Zr metal, O_2 gas and ZrO_2 is presumably established, without "suboxide" formation. The presence of carbon can lead to the temporary formation of carbides. These compounds will all eventually decompose in an oxidizing environment. The biggest problem in the use of carbon rings is, however, the necessary evolution of gases as the carbon is oxidized. This usually takes place smoothly. However, with BaZrO_3 there is a pronounced tendency to freeze over the top surface of the melt because of heat losses there by radiation, convection, etc. If the surface does freeze over the gases may be trapped below. This is

hazardous and can result in explosive eruptions from the system when the pressure gets high. Several attempts have been made to circumvent this problem. In one approach a carbon tube was used, externally supported so that it could be held at the top of the melt where the gases could escape easily, and then later removed. This method fails because the large heat leak makes it impossible to heat the carbon sufficiently. Supporting a carbon ring on slender rods of carbon also did not work because the rods would form hot spots and oxidize rapidly.

A completely different approach was, therefore, tried for starting BaZrO_3 . Special samples of electrically conductive ceramic ZrO_2 were obtained from the Zirconium Corporation of America. These were imbedded in the power charge where they could act as susceptors. However, the conductance of these ceramics is only high at temperatures in excess of ca. 1000°C . Thus a preheating was still necessary. We attempted to achieve this by inserting a platinum metal susceptor inside the zirconia tube or ring. The intention was to heat the platinum susceptor by induction until the platinum heated the zirconia tube sufficiently so that the coupling was transferred to it. The platinum would then be removed and the zirconia tube heated by induction until fusion of the BaZrO_3 charge occurred. Despite several attempts we were not able to heat the zirconia sufficiently to act as a susceptor. Even when the zirconia was apparently above 1000°C we could not make it couple, possibly due to thermal cracking of the tubing which was apparent in certain tests. The method was not pursued further. Such a procedure may yet be possible but it is difficult. One cause of the difficulty is that the container geometry and oscillator coil, etc. are designed for efficient coupling to poor conductors. The filling factors of the platinum and the zirconia are both necessarily small and despite the large available power the coupling to the platinum is very poor. This could be greatly improved by lowering the frequency but then the zirconia and the melt (when formed) would be poorly coupled. Carbon was tried as a preheating susceptor and it did work much better than the platinum but we were still unable to couple enough energy to the zirconia to make it a susceptor.

Finally, rings of tungsten metal have been used to initiate melts of BaZrO_3 . The starting procedure was not difficult with tungsten. The high melting point of tungsten

keeps the ring intact until the BaZrO_3 has fused. The tungsten is gradually oxidized and the metal eventually vanishes. The contamination of the melt with tungstates remains a problem for crystal growing. The volatility of the oxides may be sufficient to largely remove the tungsten from the melt after a reasonable period, but so far we have always found moderate amounts of tungsten in emission spectra of BaZrO_3 fusions initiated by tungsten rings.

V. EXPERIMENTAL RESULTS AND MATERIALS

A. Analysis of Verneuil-Grown, Mn-doped SrTiO₃:

Early in this contract a number of crystals of SrTiO₃ were grown by the Verneuil process. Several of these crystals were doped with MnO₂. It had been hoped that Mn⁺⁴ would substitute for Ti⁺⁴ in the SrTiO₃ lattice. These crystals did not, however, exhibit the desired fluorescence of Mn⁺⁴, and it was very doubtful that the manganese had stayed in the tetravalent state. Two of these crystals have now been examined by electron spin resonance (ESR) in order to ascertain the valence state of the manganese. These examinations were made for us by Dr. Paul H. Kasai of the Union Carbide Research Institute. Strong ESR signals were obtained for Mn⁺² but none were seen for Mn⁺⁴. The ESR spectra were integrated to obtain a quantitative estimation. The results of this analysis are as follows:

<u>Sample No.</u>	<u>Feed Power Composition</u>	<u>Chemical Analysis</u>	<u>ESR</u>
1859-92	1% Mn	0.12% Mn	.06 - .12% Mn ⁺²
1993-12	0.02% Mn		.002 - .004% Mn ⁺²

These analyses confirm that essentially all of the manganese is present in the divalent state. This is not at all surprising since the vapor pressure of oxygen over MnO₂ increases to very high values at high temperatures. Furthermore, the oxygen vacancy mechanism in SrTiO₃ can supply electrons for the reduction of the manganese. The ESR analyses do not indicate whether the Mn⁺² is in the A-site (Sr) or the B-site (Ti).

B. Summary of Skull-Melting Experiments:

The experimental conditions and observations for most of the skull-melting experiments have been briefly summarized and collected in Table II. Information about the coil, the type of container, the operating frequency, the duration of the melt and pertinent other remarks are included. The table is self-explanatory and shows the chronological development of skull-melting, and the achievements and difficulties encountered in the individual experiments. The experimental problems have been treated above. It is

convenient here to discuss the results in terms of the particular oxide systems.

Titanates: SrTiO_3 and BaTiO_3 : While these compounds, particularly SrTiO_3 , may be of some interest as symmetric laser host candidates, our main purpose was to use them as pilot substances for studying the skull-melting, since they are much less refractory than BaZrO_3 . This choice may have been somewhat unfortunate, since it now appears that they behave rather differently than BaZrO_3 . These compounds have been fused in several of the experimental geometries and melt durations of up to seven hours have been achieved. To date, we have had no indication that these melts could not be sustained indefinitely. The skull boundary is somewhat adjustable by altering the r-f power and the melts were always mobile and flowing from edge to center as shown in Figure 7. This is as expected for a small "skin depth" where only the outer regions of the liquid act as a susceptor. This pumps the liquid up on the outside and down in the center. This flow pattern is very similar to that obtained with crucibles and should be amenable to crystal pulling and we have pulled polycrystalline masses of SrTiO_3 such as shown in Figure 8. Examination of these masses shows many small crystallites and a dark color indicative of oxygen deficiency. It is almost certain that this oxygen deficiency creates electronic defects which absorb radiant energy from the melt. The material being "pulled" then acts as a thermal insulator and impedes further growth. It is very difficult if not truly impossible to pull single crystals under these conditions.

The experiments with BaTiO_3 (2146-66 and 68) were performed in order to study the effect of charge compensators on the mass pulled from the melt. Only a black polycrystalline mass was pulled from pure BaTiO_3 . A small quantity of La_2O_3 was then added to the melt and pulling again attempted. A very black misshapen mass was pulled. Such doping is known to produce an n-type semiconductor (see above). The experiment seemed to confirm our predictions that such a defect is detrimental to crystal formation. The container was emptied and recharged with BaTiO_3 . After starting the melt a small quantity of Al_2O_3 was added. This type of doping should increase the oxygen deficiency but decrease the electronic defects. The pulled mass was indeed lighter in color than pure or La-doped BaTiO_3 . It was, however, still opaque and rather dark. There was little

evidence that such compositions could be induced to grow in a manner where a single crystal would dominate.

One rather obvious way to decrease the oxygen deficiency is to increase the oxygen partial pressure. Early experiments showed that this did not help the formation of single crystals. The solubility of oxygen in the liquid is apparently rather high and this excess oxygen is rejected at the liquid solid interface where the mass is being pulled. This is a further impediment to heat transfer. Under these conditions the pulled mass tends to be concave or "hollow".

Alumina: Al_2O_3 : The behavior of alumina is quite different from that of the titanates. We have no interest in alumina crystals (sapphire or ruby) under this contract and it was chosen only as a test substance for skull-melting. Alumina differs from the titanates in that the pulling of large single crystals is a well known art. There is no difficulty from electronic defects. It should, therefore, be possible to pull crystals from skull-melted alumina.

The alumina melts were initiated with carbon rings. The process proceeded smoothly. Unlike BaZrO_3 there seemed to be little tendency to freeze over. In fact, several "blow holes" tend to form in the charge before it is completely fused, apparently kept open by the escaping oxides of carbon. These holes cannot be blocked by adding powder. There is evidence of a partial reduction of the Al_2O_3 by the carbon but after running a while in an oxidizing atmosphere, the carbon is apparently completely oxidized and removed.

The behavior of the melt is considerably different than that of the titanates. First of all, a greater driving power is required to maintain the melt. After the initial fusion, where the carbon is still present and the melt is quite turbulent, the liquid becomes more quiet and eventually appears to be nearly stagnant. The surface temperature becomes quite uniform and the surface of the liquid becomes uniformly bright. In fact, it becomes very difficult to "see" the surface for there is nothing to see and it appears blurred. This type behavior is only to be expected when the "skin depth" becomes very thick, corresponding to a small F-value where the coupling is very poor. The geometry was such that the only reasonable explanation was a gross decrease in the electrical conductivity of the melt.

This prompted us to make the separate measurements of the conductivity of Al_2O_3 reported in the Appendix. The value of the conductivity, 384 mho/m, is but one-fourth the previously accepted value but not low enough to readily explain the poor coupling observed. The skull-melting experiments were performed in the open air, while the atmosphere in which the conductance measurements were made was probably less oxidizing. The effect of the electrodes (iridium) also cannot be discounted. Further experiments would be required to determine the true conductivity of Al_2O_3 melts and its dependence on atmospheric composition.

Whatever the cause, the experimental effect is that continually greater driving currents are required to maintain the melt. Eventually the current required becomes more than the oscillator can supply (ie. the maximum plate voltage of the oscillator tube has been reached). Gradually, the melt will freeze terminating the experiment. Even so, one of the Al_2O_3 melts has been kept for three hours and appeared at the time to be stable, as noted in Table II. However, all the experiments with Al_2O_3 melts were eventually terminated because of eventual difficulty in sustaining the melt.

The only way to cure the problem of poor coupling that is encountered with Al_2O_3 melts is by changing the design so as to increase the value of F . While it may be possible to alter the electrical conductivity of the melt by dopants or by control of the gaseous "atmosphere", this procedure would not usually conform to the requirements of growing crystals from "pure" oxide melts. The only other ways to increase F are by increasing the size or raising the frequency. These two parameters are related, for the inductance of a coil and therefore its operating frequency, are dependent on its size. Furthermore, increasing the frequency by decreasing the tank-circuit capacitance is of little benefit, since the circulating current is decreased and the delivered power may drop. For these and other empirical reasons, we have found it impractical to elevate the oscillator frequency much above 3 megacycles. Consequently, the only practical cure for poor coupling appears to be to increase the size of the apparatus, while simultaneously employing a coil geometry which results in a low inductance and therefore does not greatly decrease the frequency. This is what we attempted to do in constructing the container labeled HDC No. 2 in Table II.

The internal diameter of this container is five inches which may be compared to 2.5-inches for HDC No. 1. The increase in area and thus in F should be a factor of 4.

In the experiment described by Monteforte,⁽¹⁷⁾ a water-cooled-copper can was soldered to the coil as a bottom. Sterling and Warren⁽¹⁸⁾ used a variety of container shapes; their "cage crucible" was an inverted dome made of arcs of silver tubing. At the lower end the tubing converged and connected to two isolated manifolds, thus forming a sort of "bottom" for the charge. In our experiments, the desirability of having a bottom had been noted, because with merely the powder charge the melt gradually tends to sink, (but should eventually stabilize). The bottom would aid in this stabilization. We, therefore, machined HDC No. 2 so that the "leaves" converged to form a bottom for the charge. As the table shows, this container did not perform as desired. The cause is almost certainly the bottom. The electrical behavior (capacitance, self-resonance, etc.) was inferior to the straight cylinders, and melts could neither be started or maintained in it. In order to proceed further, the bottom would have to be machined out or a new large container built. At present it remains an open question whether or not Al_2O_3 can be kept molten in a container of this size.

Barium Zirconate BaZrO_3 : This compound is the most difficult to fuse. Unlike the two other systems, starting the melt is a severe problem. Of the many methods tried, we have had consistent results only with carbon and tungsten starting rings. Even with these there are problems. The gas evolution that occurs with carbon causes a hazard and also makes the operation difficult to reproduce, while tungsten acts as an impurity.

Once the melt is formed, coupling of electrical power to the liquid occurs without apparent difficulty, at least in the early stages. However, the high temperature ($>2600^\circ\text{C}$) and the consequently large radiation from the top surface of the melt, make the heat losses large. A large driving power is required to keep the melt from freezing over on the top. The radiative losses will increase with the cross-sectional area of the apparatus. The container HDC No. 1 was made with internal diameter of only 2.5-inches because, at the time, this was thought to be about as large a radiation surface that we could maintain with the available power.

The skull-melting experiments with BaZrO_3 have been alternately encouraging and frustrating. Melts have been maintained for as long as 3 hours (2146-12) and attempts to pull crystals were apparently impeded more by lack of a seed crystal than by control of the melt. However, the experience with BaZrO_3 seems to be parallel to that of Al_2O_3 . Eventually the melts become quiescent and of uniform temperature, indicative of large skin depth and poor coupling. These observations foretell the termination of the experiment. Presumably, the poor coupling here is also the result of a decrease in the electrical conductivity of the melt. As with Al_2O_3 , a better result would be expected in a larger apparatus but with BaZrO_3 we cannot get much larger without increasing the radiation power excessively.

The problem encountered in BaZrO_3 and Al_2O_3 appear to be attributable to changes in the electrical conductivity of the liquid. This may be a fundamental problem in skull-melting of oxides, though our experiments fall short of proving this. However, in most "conductors" or "susceptors" the charge carriers are electrons (or holes) whose concentration and mobility is determined by the "intrinsic" structure of the material. The charge carrying species in molten oxides are not known, nor is it known whether they are "intrinsic" or "extrinsic" in origin. The evidence seems to indicate that gross changes in conductivity may occur during the course of an experiment, making it difficult to attribute the conductance exclusively to intrinsic processes. This problem must be resolved before the skull-melting process can be practically exploited in the synthesis of BaZrO_3 and other dielectric oxides.

REFERENCES

- (1) F. Forrat, R. Jansen and P. Trévoux, Comptes Rendus, Acad. Sci. t 256 1271 (1963).
- (2) "Laser Materials" Final Report - Korad Corporation No. AD439901, April, 1965.
- (3) C. D. Brandle, H. Fay and O. H. Nestor, Czochralski Growth of LaAlO_3 , Union Carbide Corp., Linde Division, Speedway Laboratories No. SRCR-65-4 July, 1965
- (4) G. J. Goldsmith and H. L. Pinch, "Divalent Rare Earths in Optical Maser Materials", Radio Corporation of America, Technical Report AFML-TR-65-115, April, 1965.
- (5) H. Fay, C. D. Brandle and O. H. Nestor, "Symmetrical Laser Crystals" Semiannual Technical Summary Report, Union Carbide Corporation, Linde Division, Speedway Laboratories, No. SRCR-65-2.
- (6) A. F. Devonshire, Advances in Physics 3 85 (1954)
- (7) R. O. Bell and G. Rupprecht, Phys. Rev. 129 90 (1963)
- (8) J. Koenig and B. Jaffe, J. Am. Ceram. Soc. 47 87 (1964)
- (9) E. J. W. Verwey, "Oxidic Semi-Conductors" p. 151 in "Semiconducting Materials", Butterworths, London, 1951.
- (10) Reference 4, p. 29.
- (11) Reference 4, p. 4 and 6.
- (12) R. C. McMaster, editor, "Nondestructive Testing Handbook", Vol. II, Chapters 36 and 37, The Roland Press Co., New York, 1959.
- (13) F. Föhrster et al., Z. für Metallkunde 45 166, 171, 197, 206 and 221 (1954).
- (14) Reference 12, Section 36, page 15; and reference 13 pages 166 to 171.
- (15) Reference 12 Section 36, page 20.
- (16) A. E. van Arkel, E. A. Flood and N. F. H. Bright, Can. J. Chem. 31 1009 (1953).
- (17) F. R. Monteforte, F. W. Swanekamp and L. G. van Uitert, J. App. Phys. 32 959 (1961).
- (18) H. F. Sterling and R. W. Warren, Metallurgia 67 301 (1963).

TABLE I
COMPLEX EFFECTIVE PERMEABILITY
for full circular cylinders

<u>F</u>	<u>K'</u>	<u>K''</u>	<u>F</u>	<u>K'</u>	<u>K''</u>
0	1.0000	0.0000	9	.4990	.3599
.25	.9989	.0311	10	.4678	.3494
.50	.9948	.0620	12	.4202	.3284
1.00	.9798	.1216	15	.3701	.3004
1.44	.9592	.1700	20	.3180	.2657
2.00	.9264	.2234	36	.2367	.2070
2.56	.8857	.2698	50	.2007	.1795
3.00	.8525	.2983	64	.1772	.1608
3.24	.8332	.3121	100	.1416	.1313
4.00	.7738	.3449	150	.1156	.1087
5.00	.6992	.3689	200	.1001	.0950
6.00	.6360	.3770	400	.0707	.0682
6.25	.6216	.3775	1000	.0447	.0437
7.00	.5807	.3757	1600	.0354	.0347
8.00	.5361	.3692	10000	.0141	.0140

$$F = \frac{\sigma d^2 f}{5.066 \times 10^5}$$

where: σ = conductivity mho/m
 d = object diameter m
 f = frequency cps

$\mu^* = \mu_0 K^* = \mu_0 (K' - jK'')$ = Complex effective permeability

TABLE II (continued)
SUMMARY OF SKULL-MELTING EXPERIMENTS

<u>Material</u>	<u>Coil</u>	<u>Frequency</u>	<u>Container</u>	<u>Duration of Melt</u>	<u>Remarks</u>	<u>Ref.</u>
SrTiO ₃	5 turn 5" ID	2.49 Mc	Vert. Triangle	short	Melt leaked out-shut down.	2146-5
SrTiO ₃	5 turn 5" ID	ca. 2.5 Mc	Vert. Triangle	1.5 hrs.	Pulled for 40 min. Eu doping (2146-6-24)	2146-6
SrTiO ₃	5 turn 5" ID	ca. 2.5 Mc	Vert. Triangle	-----	Tried to restart previous run, unsuccessful.	2146-8
SrTiO ₃	5 turn 5" ID	ca. 2.5 Mc	Vert. Triangle	7 hrs.	Pulled crystalline material (2146-9-26)	2146-9
SrTiO ₃		ca. 2.5 Mc	Vert. Triangle	3 hrs.	Melted on top of previous run. Pulled material (2146-11-15) Sm doping.	2146-11
BaZrO ₃	5 turn 5 1/2" ID	ca. 2.5 Mc	Vert. Triangle	3 hrs.	Stable melt of BaZrO ₃ . Attempt to pull material on ZrO ₂ rod not successful.	2146-12
BaZrO ₃		ca. 2.5 Mc	Vert. Triangle	short	Melt too low-lost coupling.	2146-13
SrTiO ₃	5 turn 6" ID	ca. 2.5 Mc	Vert. Triangle	5 hrs.	Good melt. Attempt to pull on seed. Testing control.	2146-15
SrTiO ₃	5 turn 5" ID	2.67 Mc	Modified Vert. Triangle	5 hrs.	Shielded Coil-Plate current control. Attempt to pull-lost due to setting current too low.	2146-41
BaZrO ₃	5 turn 5" ID	2.87 Mc	Modified Vert. Triangle	short	Short run due to gas entrapment. Melt forced out violently-Aborted.	2146-51
BaZrO ₃	4 turn 5" ID	3.36 Mc	HDC No. 1	Wouldn't melt	Try to start by heating ZrO ₂ ring with Graphite Rod until ZrO ₂ couples	2146-63
Al ₂ O ₃	4 turn 5" ID		HDC No. 1	3 hours	Stable melt of Al ₂ O ₃ , but too hot to pull, except small dia. (1/16") crystal.	2146-64

TABLE II
SUMMARY OF SKULL-MELTING EXPERIMENTS

<u>Material</u>	<u>Coil</u>	<u>Frequency</u>	<u>Container</u>	<u>Duration of Melt</u>	<u>Remarks</u>	<u>Ref.</u>
SrTiO ₃	10 turn 5" ID 3/8" tubing	310 Kc	Horiz. "C" boat	2.5 hrs.	Start with Ti ring. Melted 3 kg. "Cubes" of SrTiO ₃ in cooled mass.	1996-44
BaZrO ₃	10 turn 5" ID	308 Kc	Horiz. "C" boat	1 hr.	Start with Zr ring. Several starts. Attempt to cool slowly for crystals.	1996-68
BaZrO ₃	8 turn 5" ID	319 Kc	Horiz. "C" boat	-----	Unreacted powders. Abortive run. Spark and water leak.	1996-71
BaZrO ₃	8-4 and 6 turn 5" ID	8 = 321 Kc 4 = 258 Kc 6 = 258 Kc	Horiz. "C" boat	50 min.	Tried several coils. Melt only with 6 turn before shutdown.	1996-76
BaZrO ₃	6 turn 5" ID 6 turn 6 1/2" ID	341 Kc 321 Kc	Horiz. "C" boat	short	Start with carbon. Run ca. 50 min. before hole in boat. Light colored melt.	1996-78
BaZrO ₃	6 turn 6 1/2" ID	320 Kc	Horiz. "V" boat	nil	Several attempts to start without success.	1996-83 -86
SrTiO ₃	10 turn 7" ID		Special horizontal bottomless boat	short	Eventually burned through ceramic "bottom".	1996-90
SrTiO ₃	10 turn 7" ID		Modified "V"	short	Spark from coil to boat, shut down.	1996-91
SrTiO ₃	10 turn 4 1/8" ID	390 Kc	"Hollow log"	short	Start with carbon - aborted due to arc on coil.	1996-92
SrTiO ₃	8 turn 4 1/8" ID	400 Kc	"Hollow log"	short	Start with carbon-melt established but lost-poor coupling.	1996-94
SrTiO ₃	5 turn 5" ID	2.44 Mc	Vert. Triangle	2 hrs.	Good melt-attempt to pull (see photograph).	2146-1
SrTiO ₃	5 turn 5" ID	2.44 Mc	Vert. Triangle	4.5 hrs.	Good melt-pulled crystalline material on Ir rod (2146-4-26)	2146-4

FIGURE 1 -

COMPLEX EFFECTIVE PERMEABILITY

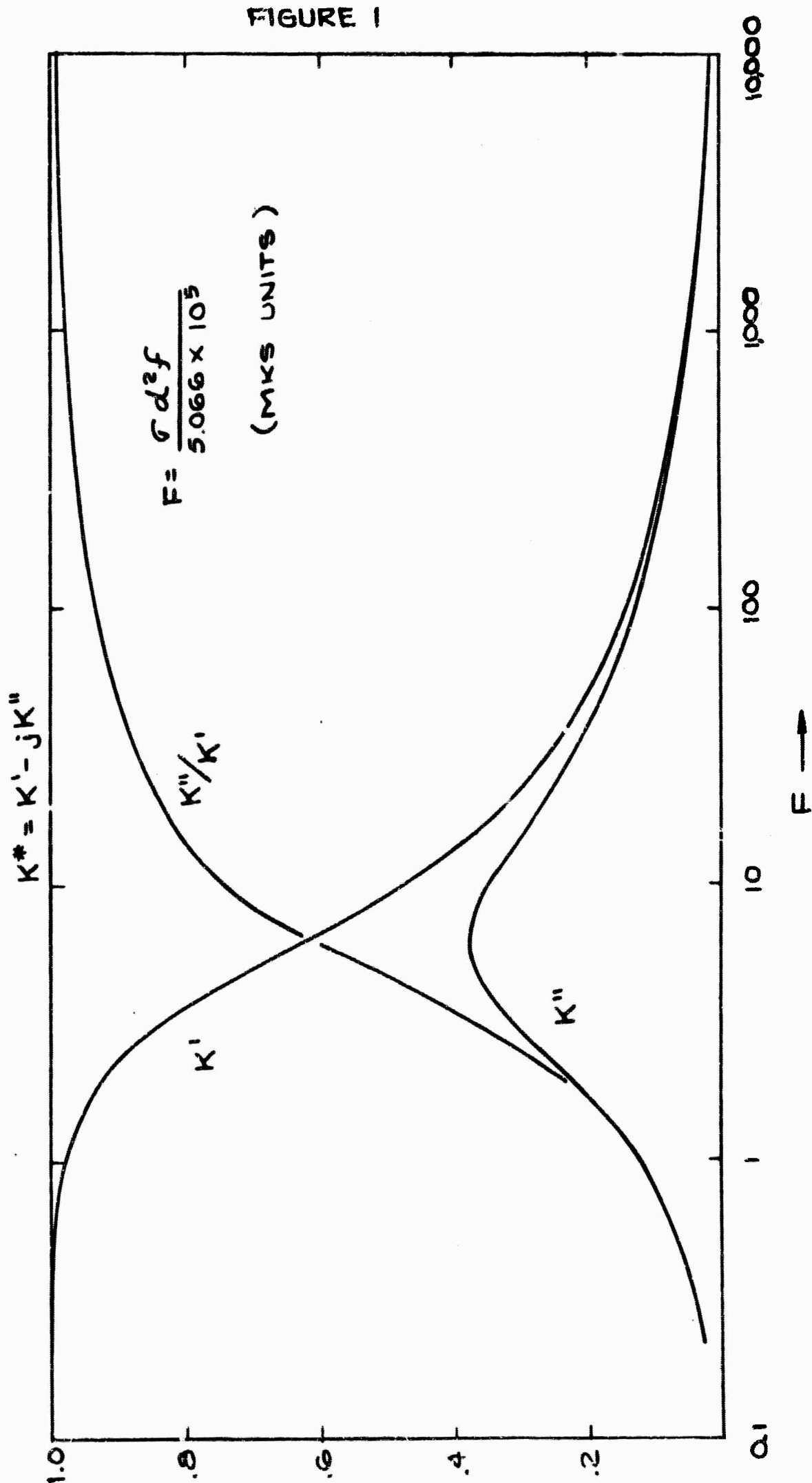


FIGURE 1

TABLE II (continued)

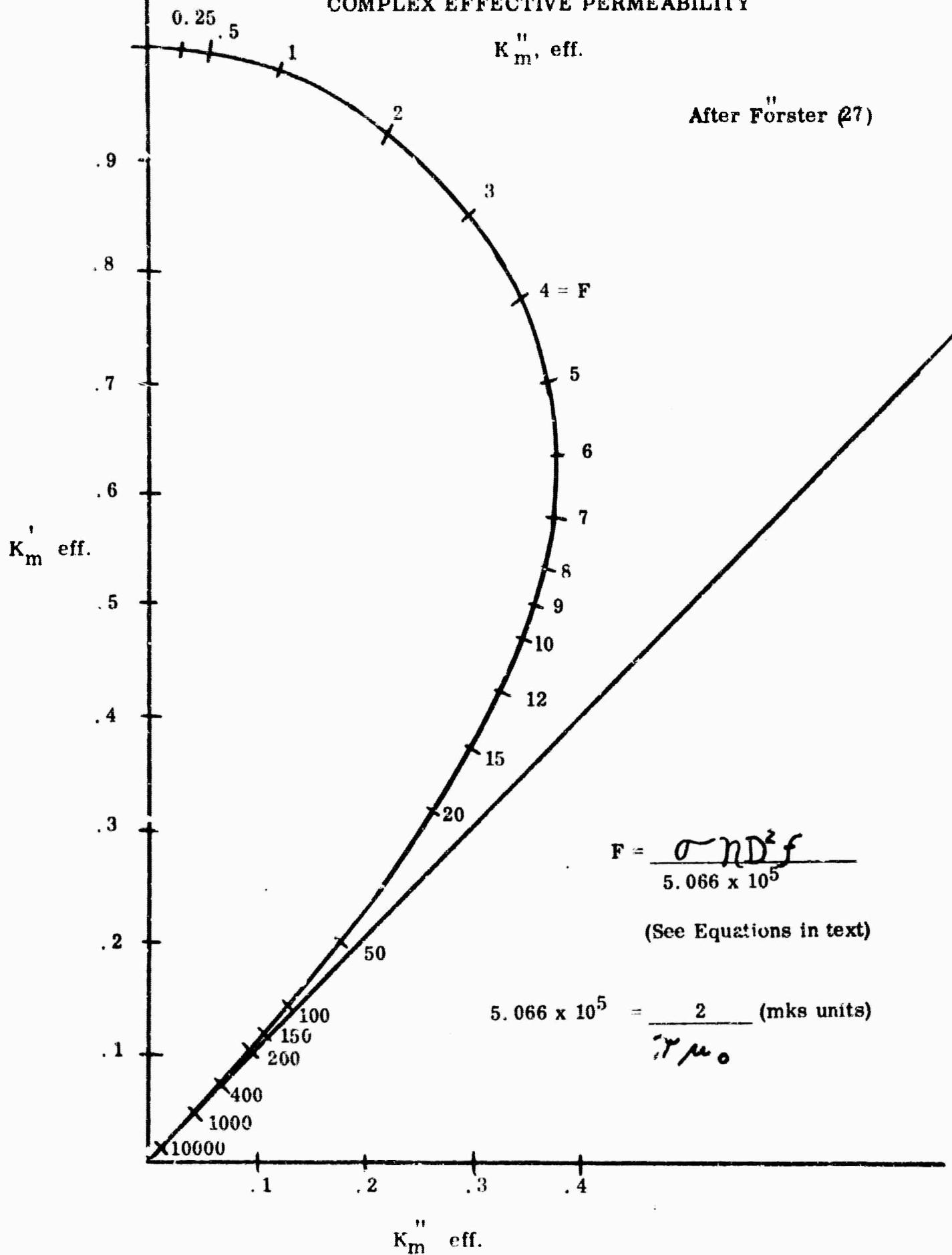
SUMMARY OF SKULL-MELTING EXPERIMENTS

<u>Material</u>	<u>Coil</u>	<u>Frequency</u>	<u>Container</u>	<u>Duration of Melt</u>	<u>Remarks</u>	<u>Ref.</u>
BaTiO ₃	4 turn 5" ID		HDC No. 1	5 hours	Stable melts, but pulling not very successful. (Black crystal). Start with Ti Metal Ring.	2146-66
BaTiO ₃	4 turn 5" ID		HDC No. 1	4 hours	Start on test No. 66 but adding dopant to aid crystal growth, same results, black crystal.	2146-68
Al ₂ O ₃	4 turn 5" ID		HDC No. 1	Short duration	Many attempts to achieve good melt.	2146-70
BaZrO ₃	4 turn 5" ID		HDC No. 1	Short	Unable to achieve melt, carbon ring.	2146-71
BaZrO ₃	4 turn 5" ID	3.0 Mc	HDC No. 1	30 minutes	W ring used to start melt, more successful, unable to maintain very long.	2146-72
BaZrO ₃ w/ ZrO ₂	4 turn 5" ID	2.98 Mc	HDC No. 1	45 minutes	W ring, 70 wt % BaZrO ₃ , 30 wt % ZrO ₂ , pull small poly-crystal. (2146-72-21).	2146-72
BaZrO ₃ w/ ZrO ₂	3 turn 5" ID	3.75 Mc	HDC No. 1	1 hr.	Same powder mixture as 2146-72 W ring, pulled out poly-crystal. material only.	2146-74
Al ₂ O ₃	3 turn 8 1/2" ID	3.2 Mc	New larger container - er HDC No. 2		Unable to start.	2146-78.
Al ₂ O ₃	3 turn 8 1/2" ID		New larger container - er HDC No. 2	Short	Started on one side of melt and melted around the circumference, but unable to achieve full melt.	2146-81
Al ₂ O ₃	3 turn 8 1/2" ID	2.12	New larger container - er HDC No. 2	Nil	About the same as previous test.	2146-82

*Containers labeled HDC 1 and HDC 2 have a cylindrical cross section similar to that shown in Figure 5. In HDC 1 the "leaves" are straight throughout their length while in HDC 2 they converge toward a point thus forming a "bottom" for the charge.

FIGURE 2

COMPLEX EFFECTIVE PERMEABILITY



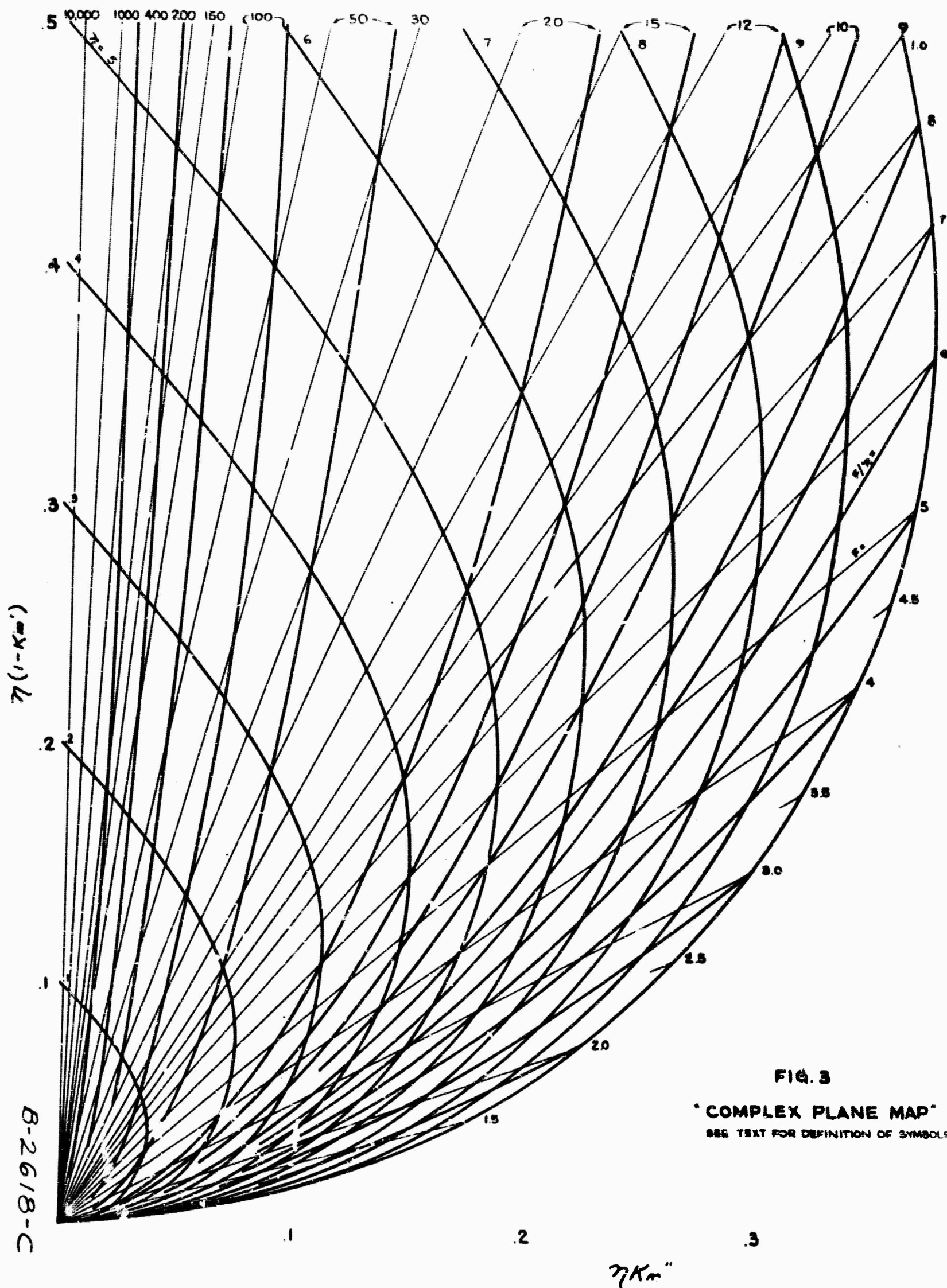
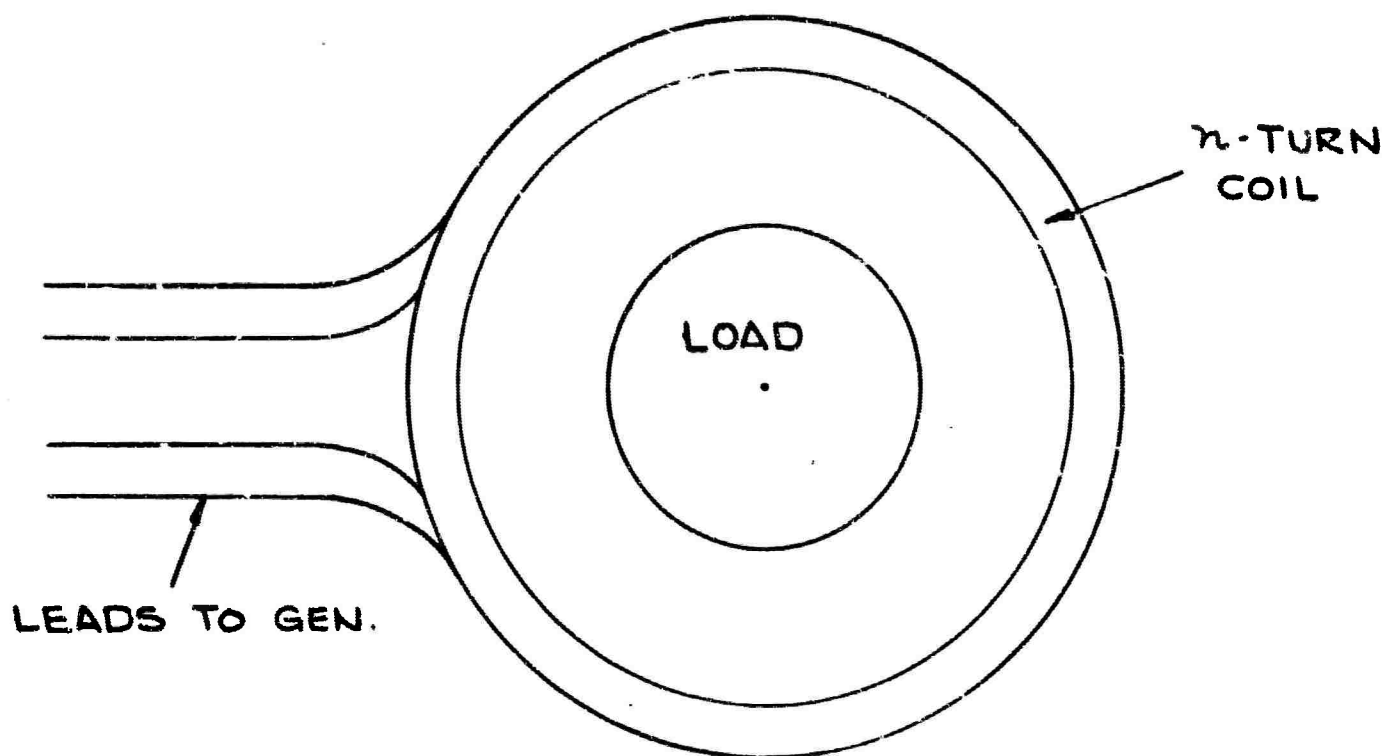


FIGURE 4 -
SIMPLE COIL AND LOAD



EQUIVALENT CIRCUIT

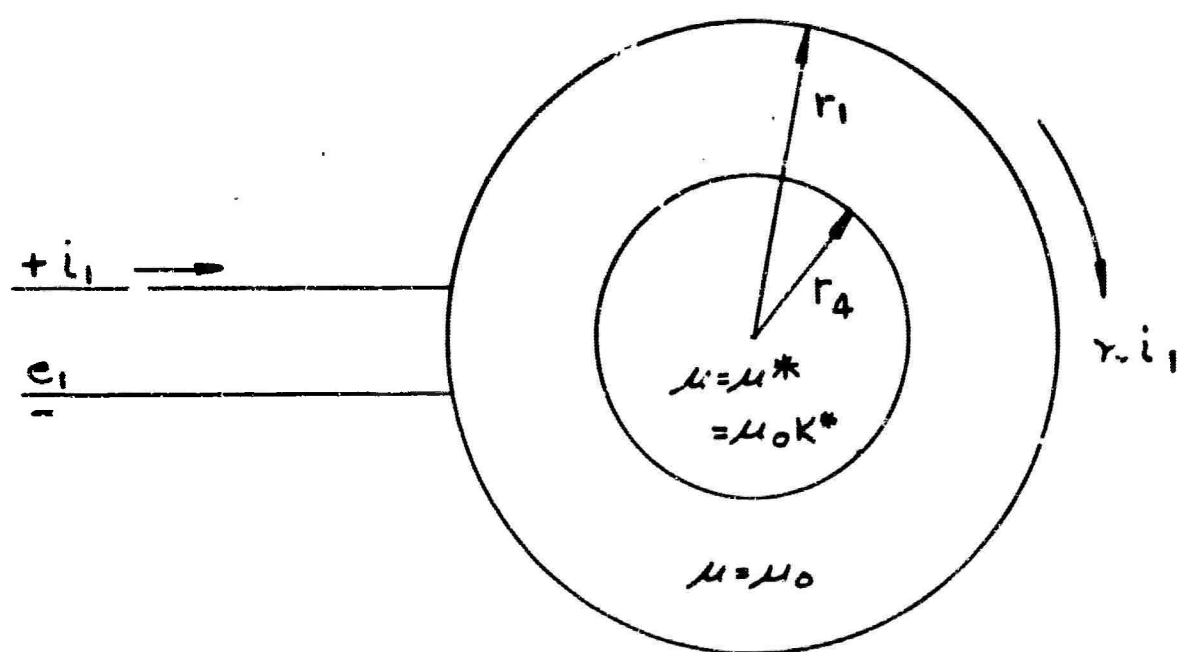
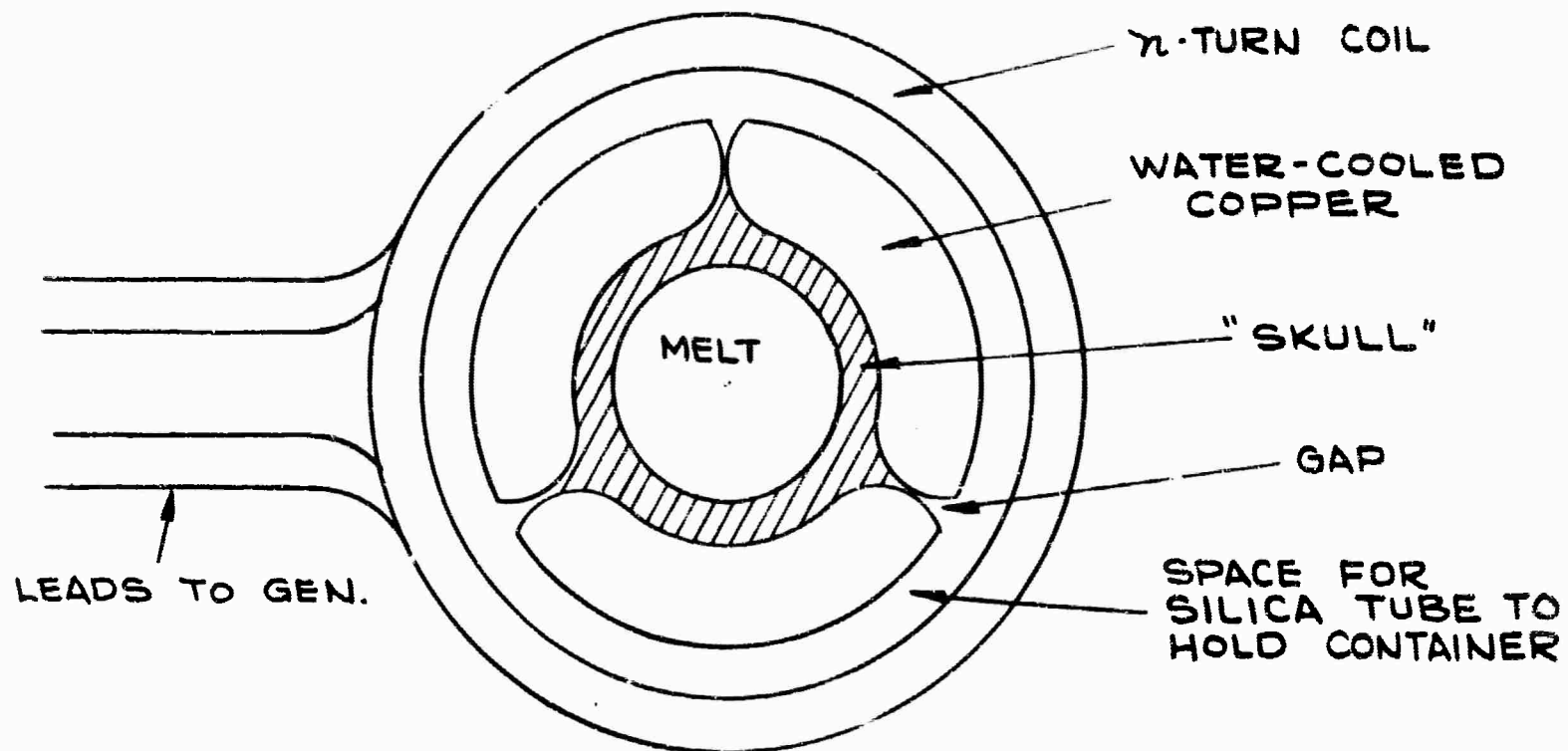


FIGURE 5 -
SKULL-MELTING COIL, VESSEL AND LOAD



EQUIVALENT CIRCUIT

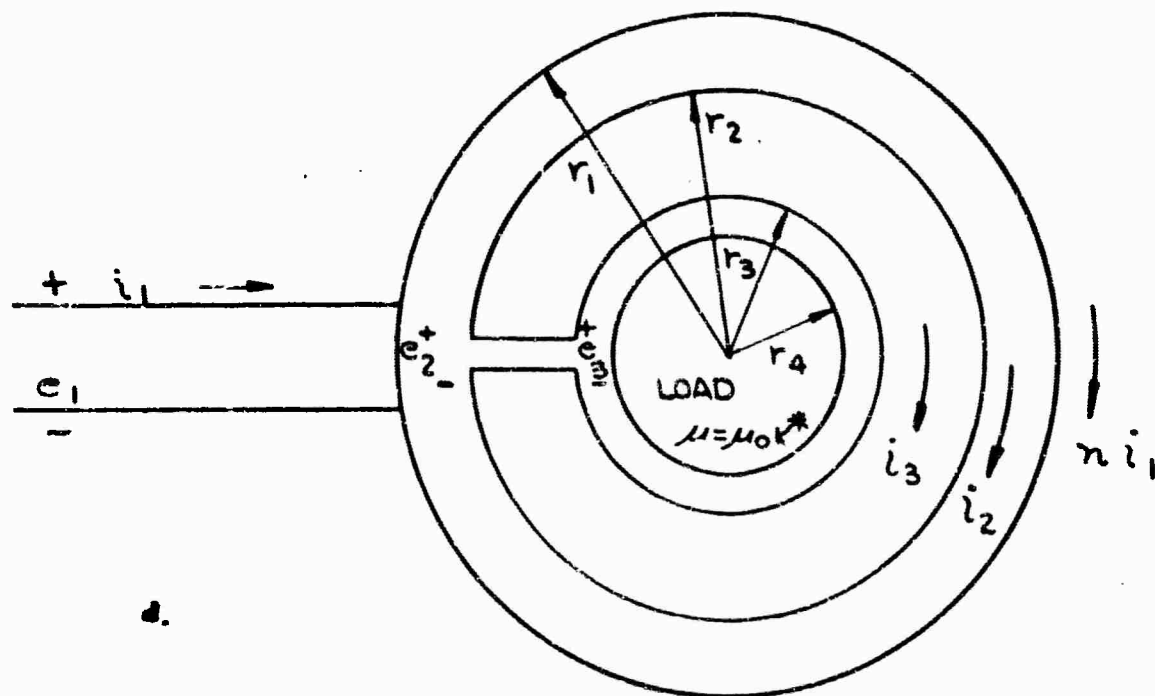


FIGURE 6

ELECTRICAL CONDUCTIVITIES OF VARIOUS SUBSTANCES
AS A FUNCTION OF $1/T$ °K

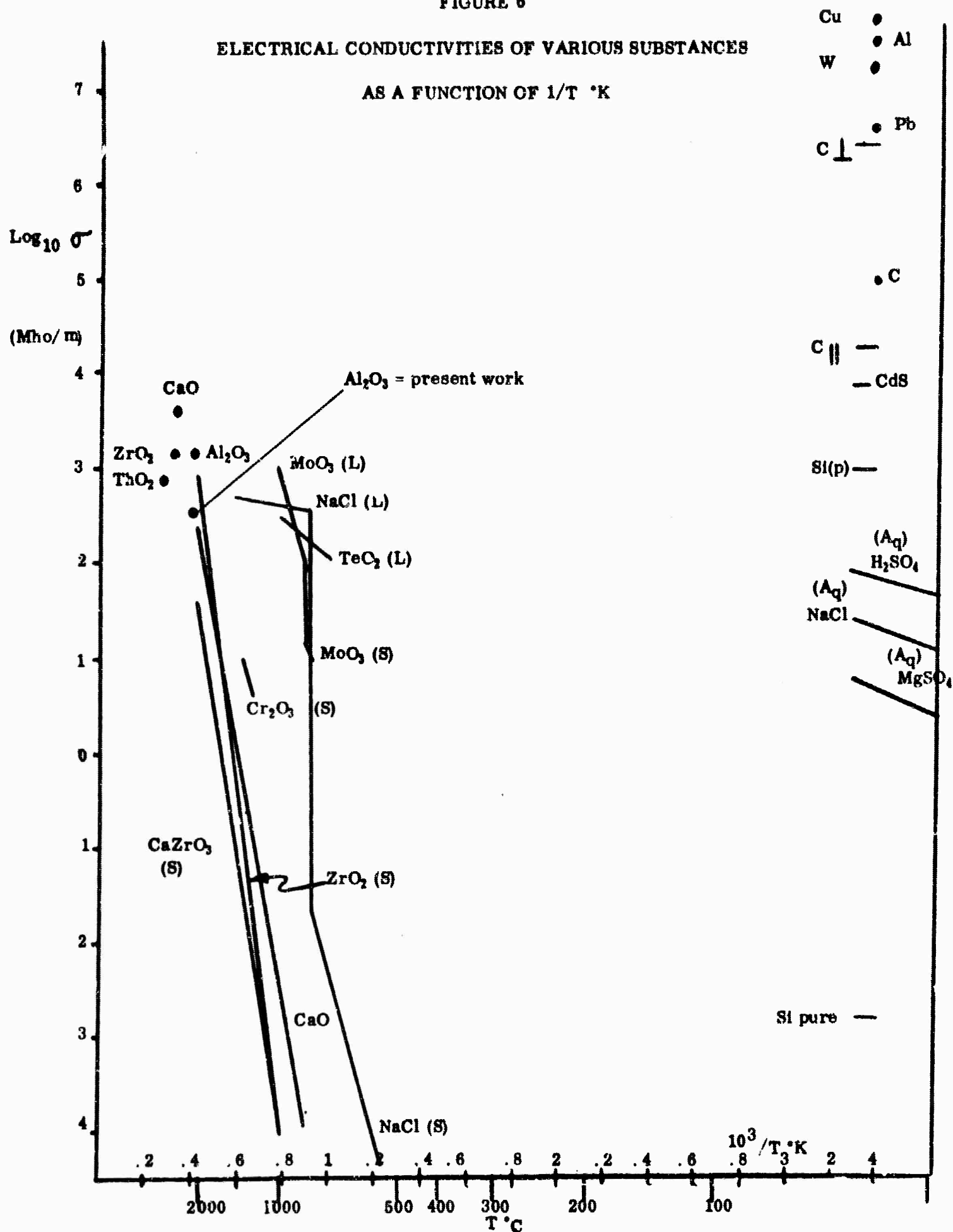
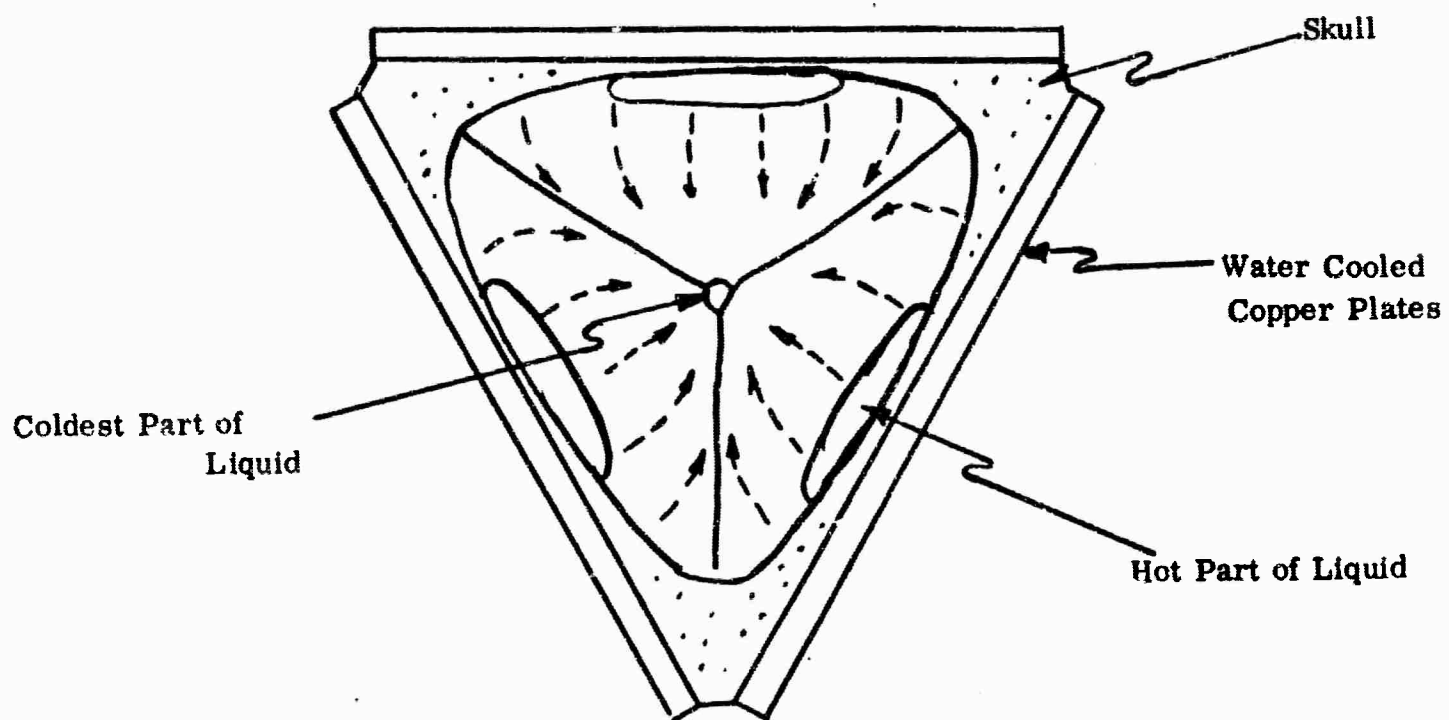


FIGURE 7
TRIANGULAR ASSEMBLY FOR SKULL-MELTING
(Schematic)

Broken Arrows Shows Direction
of Flow of Liquid



LIQUID FLOWS UP SIDES OF SKULL AND DOWN CENTER

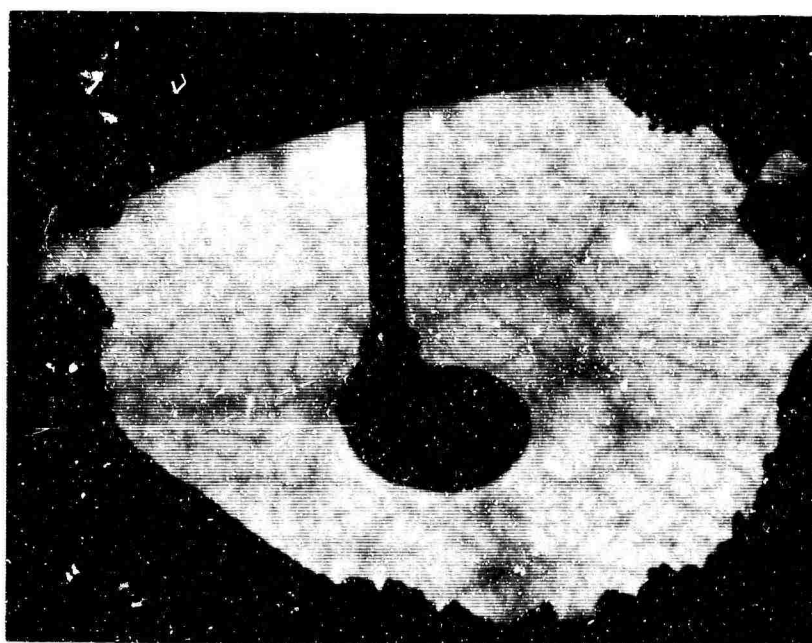
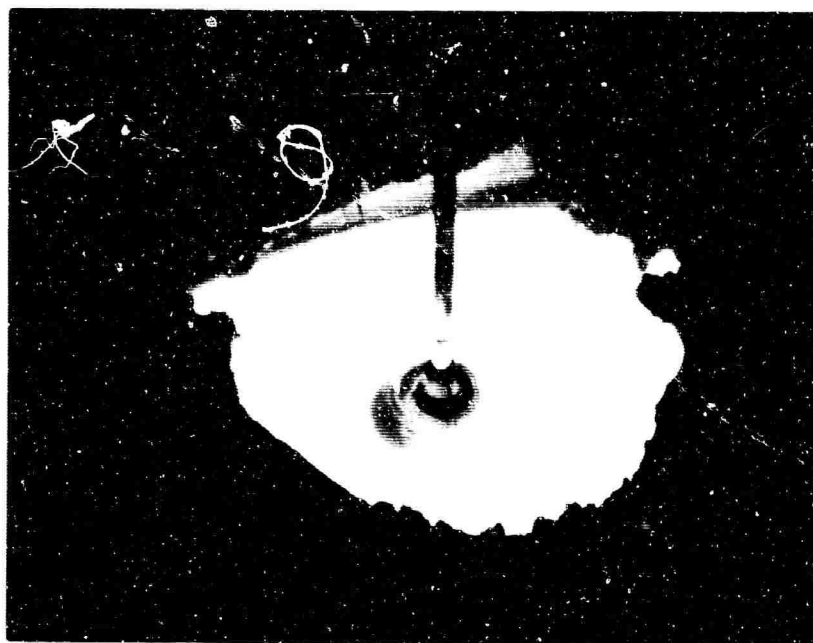


Figure 8 - Photographs of Skull Melts of SrTiO_3

APPENDIX
THE ELECTRICAL CONDUCTIVITY OF LIQUID
Al₂O₃ (MOLTEN CORUNDUM AND RUBY)

by Homer Fay
Union Carbide Corporation
Linde Division, Speedway Laboratories
Indianapolis, Indiana

ABSTRACT

The electrical conductivity of pure liquid Al₂O₃ has been measured at ca. 2400°K and found to be $384 \text{ mho m}^{-1} \pm 5\%$. This value is one-fourth that usually quoted. The measurements were made in an iridium crucible with a coaxial iridium rod as the second electrode. By measuring the resistance as a function of the immersion depth of the iridium rod, both the conductivity and the series circuit resistance were determined. The cell was calibrated with aqueous electrolyte solutions after correcting for polarization effects. The possibility that the electrical conductivity is dependent on the oxidation-reduction properties of the atmosphere is considered.

INTRODUCTION

Data on the electrical conductivity of liquid metal oxides are still quite scarce. The conductivities of the more refractive oxides in particular, have in most cases only been estimated from electric furnace measurements. Mackenzie⁽¹⁾ classifies oxide melts as either non-conducting "network liquids" or as ionic or electronic conductors. Liquid Al_2O_3 is considered to be an ionic conductor. The most comprehensive study of the conductivities of molten oxides is probably still that of van Arkel, Flood and Bright.⁽²⁾ They measured the conductivities of several of the lower melting oxides and compared them with halides. They also tabulated values for MgO , CaO , TiO_2 , ZrO_2 , ThO_2 , Cr_2O_3 and Al_2O_3 ; these, however were not measured directly but were estimated from electric furnace operations. The conductivity of Al_2O_3 at the melting point is given as $15 \times 10^2 \text{ mho m}^{-1}$.

Recently, we have been experimentally investigating the possibility of growing crystals from melts maintained by inductive coupling of radio-frequency power directly to the melt. In this process, the melt acts as its own susceptor and its conductance is very significant. Although not quantitative, these experiments have rather consistently indicated that the conductivity of Al_2O_3 was considerably lower than the values given by van Arkel. We, therefore, decided to attempt a direct measurement of the conductivity of liquid Al_2O_3 (molten corundum or white sapphire) and of this liquid doped with Cr_2O_3 (molten ruby).

(1)

J. D. Mackenzie, "Oxide Melts" in *Advances in Inorganic Chemistry and Radiochemistry*, Volume 4 pp. 293 ff, Academic Press Inc., New York, 1962.

(2)

A. E. van Arkel, E. A. Flood and Norman F. H. Bright, *Canadian J. of Chemistry* 31 1009-1019 (1953).

EXPERIMENTAL

The scarcity of high temperature conductance data is due to the difficulty of finding sufficiently inert and refractory materials to use for crucibles and electrodes. After some experimentation, an iridium crucible as one of the electrodes and a small diameter iridium rod as the other were found to be satisfactory for this purpose. A diagram of the electrode and crucible configuration is shown in Figure 1. The crucible was ca. 1.25 - inch in diameter and 1.2-inch deep but was slightly rounded on the bottom. A 2 1/4-inch diameter rim was welded to the top edge of the crucible and an iridium lead wire was welded to this rim. The crucible was supported by its rim inside a special oxy-hydrogen combustion furnace, the combustion zone being directly outside the crucible. The central iridium electrode was mounted in a Jacobs chuck of a drill press and was adjusted to be approximately coaxial with the crucible. The drill press permitted vertical movement of this electrode and measurements were made at various immersion depths as described below.

Resistance measurements were made with a General Radio Type 650A bridge driven by an internal oscillator at 1000 cps. This bridge has but a single balancing control when used for a-c resistance, and thus can measure only relatively pure resistances. A General Radio, 1000 pf variable capacitor was, therefore, inserted in the bridge in parallel with either the arm adjacent to or opposite to the unknown, as required to sharpen the balance. The bridge contained a tuned amplifier and was balanced using a Tektronix oscilloscope as the final detector. The cell was connected to the bridge through a coaxial cable, with extended lengths of bare copper wires and clips to attach to the iridium wire and to the chuck holding the iridium rod. The crucible was connected to the shield of the cable, which was grounded at the bridge. A measure of the lead resistance could be made by shorting out the leads where they connected to the iridium. This did not, however, correct the readings for the resistance of the iridium, which was not negligible. The crucible was charged with fragments of pure crystalline Al_2O_3 and heated until the charge was melted. The temperature was maintained at ca. 2400°K as measured by an optical pyrometer uncorrected for emissivity. The central iridium electrode was then lowered until it just touched the melt surface. This position was noted and identified as the "zero" position. The electrode was then lowered in 1/8-inch intervals to a depth of 3/4-inch below the zero

point. A series of resistance measurements were made with the electrode descending and later repeated as the electrode was withdrawn. (When the electrode was at a depth of 3/4-inch, a few measurements were attempted with a radio-frequency bridge. Quantitative data were not obtained but the radio-frequency measurements gave no indication of any appreciable dispersion or change in resistance with frequency). The audio-frequency measurements yielded resistance values from 0.15 to 0.38 ohms, after subtracting the lead resistance. A small but arbitrary quantity of Cr_2O_3 was then added to the charge and the measurements repeated while lowering the central electrode.

After the crucible was cooled, the crystallized ruby was removed and an estimate was made of the liquid level. The electrical assembly was then reconstructed, without the furnace, and the cell filled to the same level with nearly saturated NaCl solution. The electrical conductivity of this solution had measured with a calibrated dip cell to be 10.3 mho m^{-1} . Resistance measurements were then made as a function of immersion depth of the electrode. However, in this case the zero resistance reference point was obtained by directly contacting the crucible with the central electrode. It was found that the cell polarized quite badly when this electrolyte was used. A similar polarization had not occurred with the fused Al_2O_3 . In fact, the reactance corrections were negligibly small in the high-temperature measurements and the external capacitor was only used to sharpen the balance. Large values of external capacitance, up to a few tenths of a microfarad, were required to obtain a satisfactory balance with the electrolyte. It was, therefore, necessary to correct the bridge readings. It was assumed that the capacitive reactance was in series with the solution resistance, dielectric effects being negligibly small for this solution. The equivalent series resistance was calculated and from this the cell constant, K , was determined as a function of immersion depth. This calibration curve is shown in Figure 2. The cell constant was never "constant" but always decreased with immersion. However, the variation, over a range of depths, was smooth enough to allow reasonably accurate measurements.

The measured resistances in the Al_2O_3 experiments have been plotted as a function of the cell constant, K , as shown in Figure 3. The points should lie on a straight line since, $R = R_0 + K/\sigma$. When the data taken with the electrode descending and ascending are treated

separately, good linear fits are obtained. The two straight lines in Figure 3 have been fit by the method of least squares. The values obtained for R_0 and σ are:

	<u>R_0, ohms</u>	<u>σ, mho m^{-1}</u>
Electrode descending	0.0702	385
Electrode ascending	0.0535	383

The variation in R_0 may represent real changes in contact resistance but is more likely an effect of the meniscus at the electrode. The mean conductivity at 2400°K is:

$$\sigma = 384 \pm 8 \text{ mho/m}$$

The range limits have been calculated from an analysis of variance and represent a probable error of 2%. However, the absolute value of the cell constant is in doubt by more than this amount, and we thus estimate the conductivity to be accurate to 5%.

The addition of Cr_2O_3 to the charge caused a definite initial decrease in conductivity. As the measurements progressed, however, the resistance values for ruby approached those for pure Al_2O_3 and the last two points measured fit the average slope very well. Apparently, the conductivity was not constant during these measurements but was drifting toward an equilibrium value identical to that of pure Al_2O_3 . Finally measurements were made of the resistance of the charge as the furnace was cooled. The values of resistance increased smoothly but very rapidly as the melt solidified. The high temperature conductivity of the solid is apparently not negligible but it is still much less than that of the liquid.

DISCUSSION

The method used for measuring the conductivity of high-melting oxides in metallic crucibles appears to be capable of considerable accuracy, despite the fact that the "cell constants" are rather small and the cell must be calibrated for various immersion depths.

The conductivity of pure liquid Al_2O_3 near its melting point is, according to the present study, 384 mho m^{-1} . This is almost a factor of four lower than the value of $15 \times 10^2 \text{ mho m}^{-1}$ quoted by van Arkel.⁽²⁾ The conductivity is, however, still sufficient to consider liquid Al_2O_3 to be an ionic conductor. The charge carrying species are apparently small and mobile. No further structural inferences can be made from these few measurements. It is unfortunate that the atmospheric composition could not be controlled during these measurements. The fusion was made in the open air but the local atmosphere could have been somewhat reducing from the flame gases. Other observations indicate that the appearance of the melt, its viscosity and its conductivity may all depend on the atmosphere, reducing conditions favoring a higher conductivity. One possible mechanism that could account for such behavior is the establishment of an equilibrium between the oxygen in the atmosphere and oxygen "vacancies" in the liquid. We hope eventually to test this hypothesis by further experiments in controlled reducing and oxidizing atmospheres.

The addition of small amounts of Cr_2O_3 to the melt definitely decreases the conductivity but the effect is apparently only temporary. This further indicates that some process of equilibrium with the atmosphere is taking place.

The author thanks B. J. Corbitt for his assistance in making the measurements, and R. M. Youmans and P. V. Vittorio for making available the furnace. He also is indebted to Dr. M. N. Plooster for valuable discussions on the properties of Al_2O_3 melts, and to the Crystal Products Department of the Linde Division for permission to publish these results.

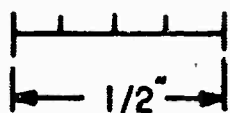
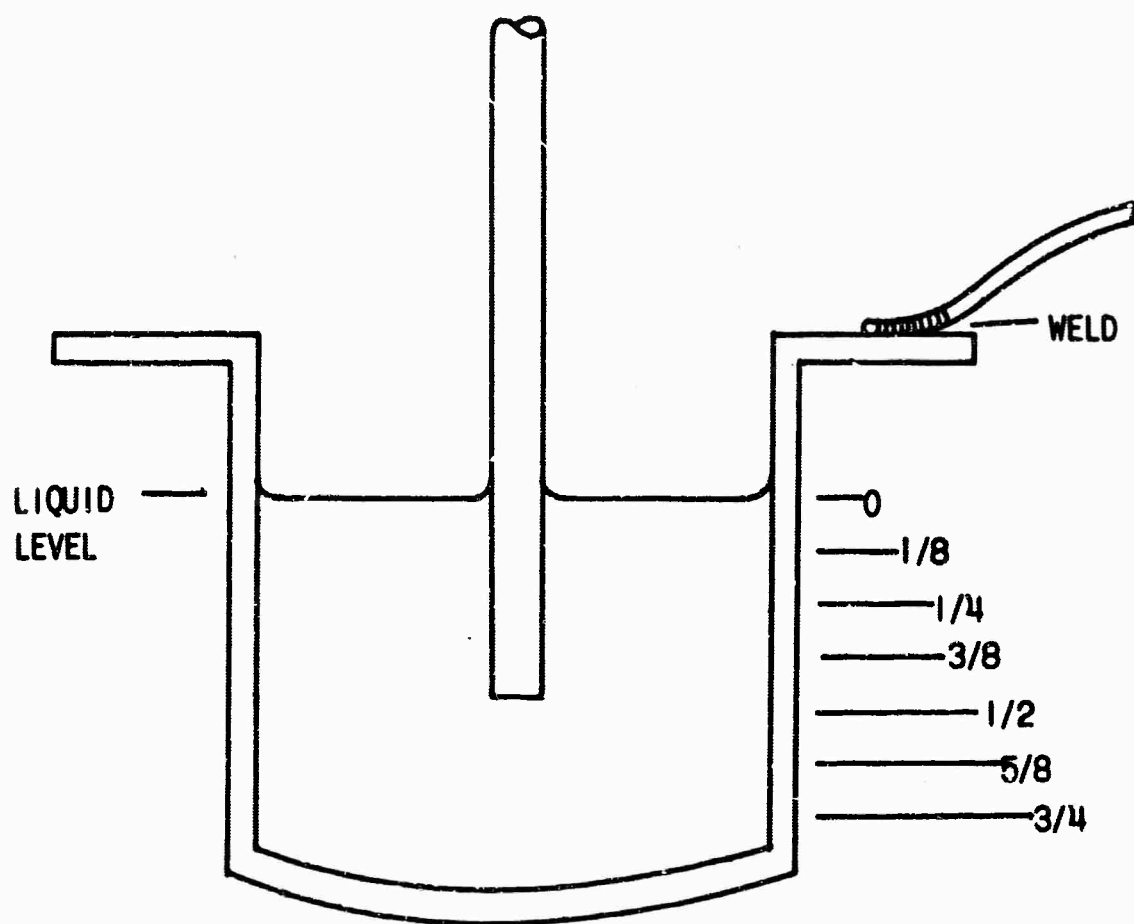


FIGURE 1
IRIDIUM CRUCIBLE AND ELECTRODE CONFIGURATION
(scale shows immersion depth in inches)

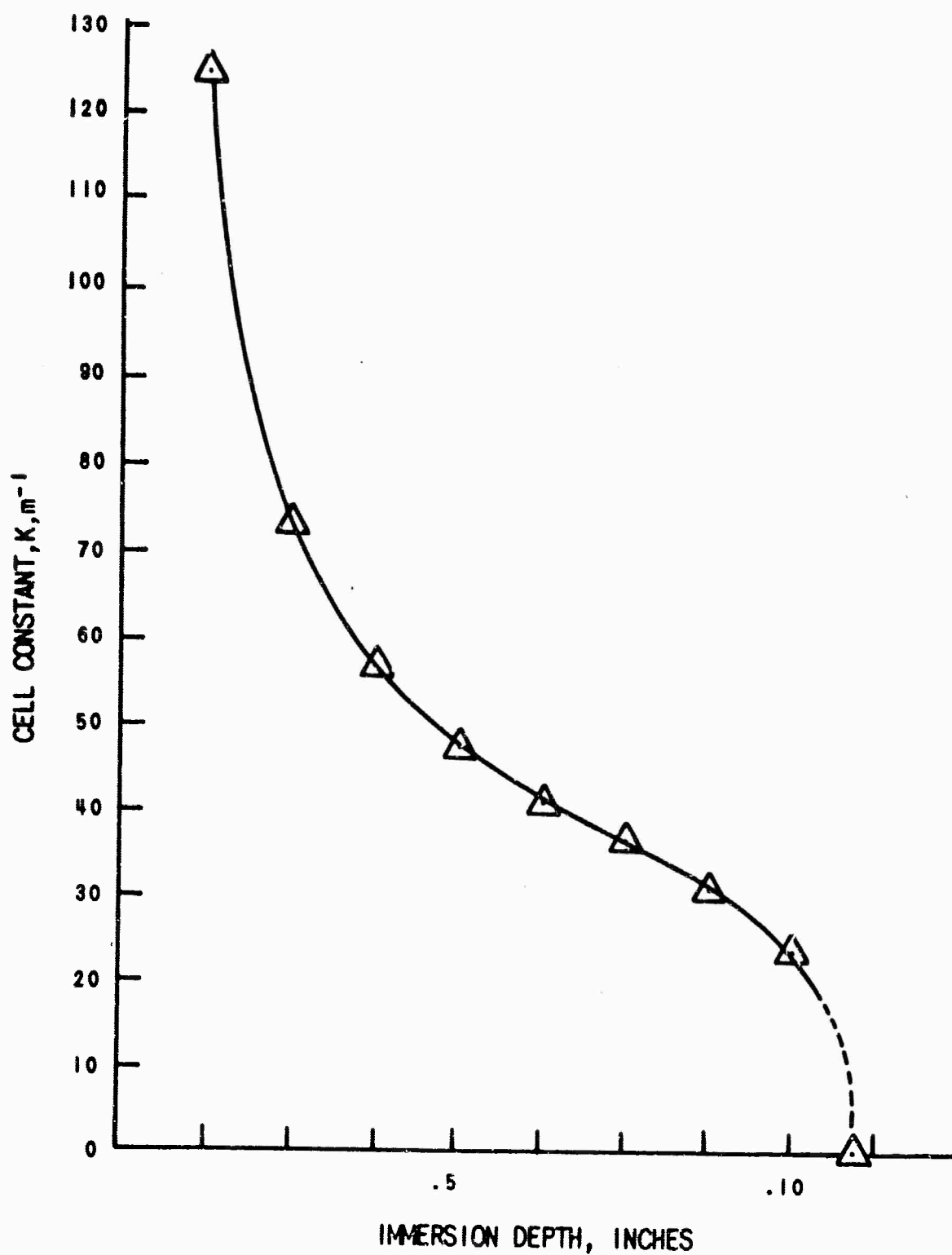


FIGURE 2
CELL CONSTANT CALIBRATION CURVE AS DETERMINED WITH AQUEOUS NaCl SOLUTIONS

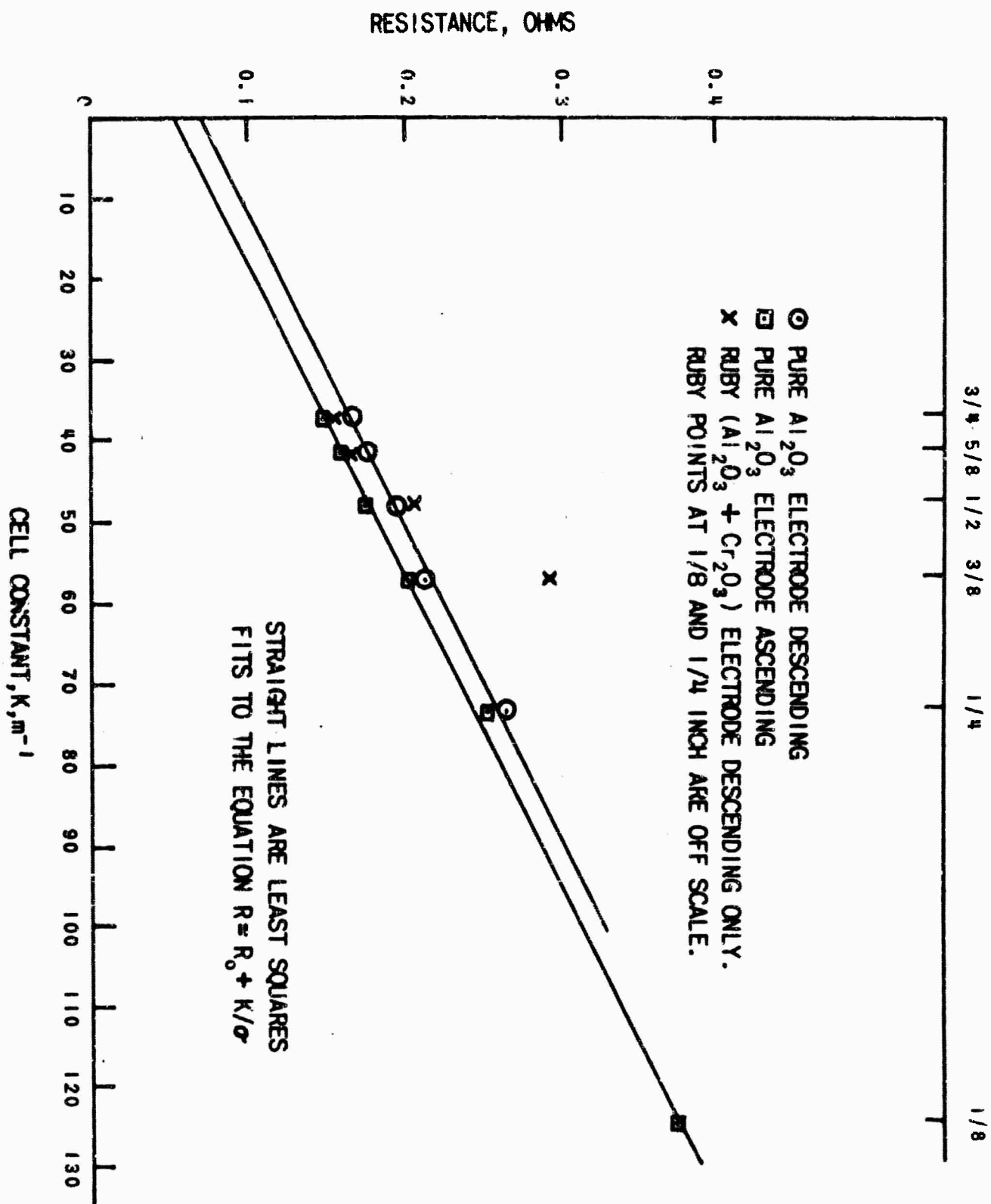


FIGURE 3
MEASURED RESISTANCE VS CELL CONSTANT FOR PURE Al_2O_3 AND RUBY AT $2400^\circ K$

1 0030	R. S. CONGLETON	54
2 0030	HUGHES AIRCRAFT CORP.	54
3 0030	AEROSPACE GROUP	54
4 0030	RESEARCH & DEVELOPMENT DIVISION	54
5 0030	CULVER CITY, CALIFORNIA	54
1 0035	BASIL CURNUTTE, JR.	54 *
2 0035	KANSAS STATE UNIVERSITY	54
3 0035	MANHATTAN, KANSAS	54
1 0042	G. H. DIEKE	54 *
2 0042	JOHNS HOPKINS UNIVERSITY	54
3 0042	BALTIMORE 18, MARYLAND	54
1 0092	C. H. KELLER	54 *
2 0092	PEK LABS, INC.	54
3 0092	925 EVELYN AVENUE	54
4 0092	SUNNYVALE, CALIFORNIA	54
1 0093	S. P. KELLER	54 *
2 0093	INTERNATIONAL BUSINESS MACHINES	54
3 0093	T. J. WATSON RESEARCH CENTER	54
4 0093	YORKTOWN HEIGHTS, NEW YORK	54
1 0108	A. LEMPICKI	54 *
2 0108	GENERAL TELEPHONE & ELECTRONICS LABS	54
3 0108	BAYSIDE 60, NEW YORK	54
1 0117	R. C. PASTOR	54 *
2 0117	KORAD CORPORATION	54
3 0117	2520 COLORADO AVENUE	54
4 0117	SANTA MONICA, CALIFORNIA	54
1 0121	T. C. MCAVOY	54 *
2 0121	CORNING GLASS WORKS	54
3 0121	CORNING, NEW YORK	54
1 0122	W. MCKUSICK	54 *
2 0122	EASTMAN KODAK COMPANY	54
3 0122	APPARATUS AND OPTICAL DIVISION	54
4 0122	400 PLYMOUTH AVENUE, N.	54
5 0122	ROCHESTER 4, NEW YORK	54
1 0139	O. H. NESTOR	54 *
2 0139	LINDE COMPANY	54
3 0139	1500 POLCO STREET	54
4 0139	INDIANAPOLIS 24, INDIANA	54
1 0144	J. W. NIELSON	54 *
2 0144	AIRTRON, A DIVISION OF LITTON INDUSTRIES	54
3 0144	200 EAST MANOVER AVENUE	54
4 0144	MORRIS PLAINS, NEW JERSEY	54

1	0148	GERALD OSTER	54 *
2	0148	CHEMISTRY DEPARTMENT	54
3	0148	POLYTECHNIC INSTITUTE OF BROOKLYN	54
4	0148	333 JAY STREET	54
5	0148	BROOKLYN 1, NEW YORK	54
1	0178	DAVID STOCKMAN	54 *
2	0178	ELECTRONICS LABORATORY	54
3	0178	GENERAL ELECTRIC COMPANY	54
4	0178	SYRACUSE, NEW YORK	54
1	0189	J. W. TURNER	54
2	0189	WESTINGHOUSE ELECTRIC CORP.	54
3	0189	ELECTRONICS DIVISION	54
4	0189	P. O. BOX 1897	54
5	0189	BALTIMORE 3, MARYLAND	54
1	0207	R. W. YOUNG	54
2	0207	AMERICAN OPTICAL COMPANY	54
3	0207	SOUTHBIDGE, MASSACHUSETTS	54
1	0213	DR. JERALD R. IZATT	54 *
2	0213	NEW MEXICO STATE UNIVERSITY	54
3	0213	UNIVERSITY PARK, NEW MEXICO	54
1	0214	PROFESSOR A. K. KAMAL	54 *
2	0214	PURDUE UNIVERSITY	54
3	0214	SCHOOL OF ELECTRICAL ENGINEERING	54
4	0214	LAFAYETTE, INDIANA	54
1	0215	MR. THOMAS C. MARSHALL	54 *
2	0215	COLUMBIA UNIVERSITY	54
3	0215	DEPT. OF ELECTRICAL ENGINEERING	54
4	0215	NEW YORK 27, NEW YORK	54
1	0216	MR. CHARLES G. NAIMAN	54 *
2	0216	MITHRAS, INC.	54
3	0216	CAMBRIDGE 39, MASSACHUSETTS	54
1	0217	DR. J. H. SCHULMAN	54 *
2	0217	SOLID STATE DIVISION	54
3	0217	U. S. NAVAL RESEARCH LABORATORY	54
4	0217	WASHINGTON 25, D. C.	54
1	0218	DR. JACK A. SOULES	54
2	0218	PHYSICS DEPARTMENT	54
3	0218	NEW MEXICO STATE UNIVERSITY	54
4	0218	UNIVERSITY PARK, NEW MEXICO	54
1	0219	DR. ARDEN SHER	54 *
2	0219	VARIAN ASSOCIATES	54
3	0219	611 HANSEN WAY	54
4	0219	PALO ALTO, CALIFORNIA	54

1	0220	PHYSICAL SCIENCES DIVISION	54
2	0220	ARMY RESEARCH OFFICE	54
3	0220	OFFICE, CHIEF, RESEARCH & DEVELOPMENT	54
4	0220	WASHINGTON 25, D. C.	54
5	0220	ATTN DR. ROBERT A. WATSON	54
1	0221	CHIEF SCIENTIST	54
2	0221	U. S. ARMY ELECTRONICS COMMAND	54
3	0221	FORT MONMOUTH, NEW JERSEY	54
4	0221	ATTN DR. HANS K. ZIEGLER	54
1	0222	DIRECTOR, INSTITUTE FOR EXPLATORY RESEARCH	54
2	0222	ARMY SIGNAL RESEARCH&DEVELOPMENT LABORATORY	54
3	0222	FORT MONMOUTH, NEW JERSEY	54
1	0223	ASST DIRECTOR OF SURVEILLANCE	54
2	0223	ARMY SIGNAL RESEARCH&DEVELOPMENT LABORATORY	54
3	0223	FORT MONMOUTH, NEW JERSEY	54
4	0223	ATTN DR. HARRISON J. MERRILL	54
1	0225	DIRECTOR OF RESEARCH & DEVELOPMENT	54
2	0225	ARMY ORDNANCE MISSILE COMMAND	54
3	0225	HUNTSVILLE, ALABAMA	54
4	0225	ATTN MR. WILLIAM D. MCKNIGHT	54
1	0226	OFFICE, CHIEF OF NAVAL OPERATIONS /OP-07T-1/	54
2	0226	DEPARTMENT OF THE NAVY	54
3	0226	WASHINGTON 25, D. C.	54
4	0226	ATTN MR. BEN ROSENBERG	54
1	0227	BUREAU OF NAVAL WEAPONS /RR-2/	54
2	0227	DEPARTMENT OF THE NAVY	54
3	0227	WASHINGTON 25, D. C.	54
4	0227	ATTN DR. C. H. HARRY	54
1	0228	BUREAU OF SHIPS /CODE 305/	54
2	0228	DEPARTMENT OF THE NAVY	54
3	0228	WASHINGTON 25, D. C.	54
4	0228	ATTN DR. JOHN HUTH	54
1	0229	OFFICE OF NAVAL RESEARCH /CODE 402C/	54
2	0229	DEPARTMENT OF THE NAVY	54
3	0229	WASHINGTON 25, D. C.	54
4	0229	ATTN DR. SIDNEY REED	54
1	0230	OFFICE OF NAVAL RESEARCH /CODE 421/	54
2	0230	DEPARTMENT OF THE NAVY	54
3	0230	WASHINGTON 25, D. C.	54
4	0230	ATTN MR. FRANK B. ISAKSON	54

03 COPIES

1 0231	OFFICE OF NAVAL RESEARCH /CODE 406T/	54
2 0231	DEPARTMENT OF THE NAVY	54
3 0231	WASHINGTON 25, D. C.	54
4 0231	ATTN MR. J. W. SMITH	54
1 0232	NAVAL RESEARCH LABORATORY /CODE 6440/	54
2 0232	DEPARTMENT OF THE NAVY	54
3 0232	WASHINGTON 25, D. C.	54
4 0232	ATTN DR. C. C. KLICK	54
1 0233	NAVAL RESEARCH LABORATORY /CODE 7360/	54
2 0233	DEPARTMENT OF THE NAVY	54
3 0233	WASHINGTON 25, D. C.	54
4 0233	ATTN DR. L. F. DRUMETER	54
1 0234	HEADQUARTERS USAF /AF DR-NU-9/	54
2 0234	DEPARTMENT OF THE AIR FORCE	54
3 0234	WASHINGTON, D. C.	54
4 0234	ATTN LTCOL TERREL	54
1 0235	RESEARCH & TECHNOLOGY DIVISION	54
2 0235	BOLLING AFB	54
3 0235	WASHINGTON, D. C.	54
4 0235	ATTN MR. ROBERT FEIK	54
1 0236	OFFICE, AEROSPACE RESEARCH /MROSP/	54
2 0236	WASHINGTON 25, D. C.	54
3 0236	ATTN LT. COL. IVAN ATKINSON	54
1 0238	TECHNICAL AREA MANAGER /760A/	54
2 0238	ADVANCED WEAPONS AERONAUTICAL SYSTEMS DIV	54
3 0238	WRIGHT-PATTERSON AFB	54
4 0238	OHIO	54
5 0238	ATTN MR. DON NEWMAN	54
1 0239	PROJECT ENGINEER /5237/	54
2 0239	AEROSPACE RADIATION WEAPONS	54
3 0239	AERONAUTICAL SYSTEMS DIVISION	54
4 0239	WRIGHT-PATTERSON AFB	54
5 0239	OHIO	54
6 0239	ATTN MR. DON LEWIS	54
1 0240	AIR FORCE SPECIAL WEAPONS CENTER /SWRPA/	54
2 0240	KIRTLAND AFB	54
3 0240	NEW MEXICO	54
4 0240	ATTN MAJOR T. T. DOSS	54
1 0241	PROJECT ENGINEER /5561/ COMET	54
2 0241	ROME AIR DEVELOPMENT CENTER	54
3 0241	GRIFFISS AFB	54
4 0241	NEW YORK	54
5 0241	ATTN MR. DURWOOD CREED	54

1	0242	DEPARTMENT OF ELECTRICAL ENGINEERING		54
2	0242	NEW YORK UNIVERSITY		54
3	0242	UNIVERSITY HEIGHTS		54
4	0242	NEW YORK, NEW YORK		54
5	0242	ATTN MR. THOMAS MENION		54
1	0243	BMDR	08 COPIES	54
2	0243	ROOM 2 R 263		54
3	0243	THE PENTAGON		54
4	0243	WASHINGTON 25, D. C.		54
5	0243	ATTN MAJOR GLENN SHERWOOD		54
1	0284	MR. JOHN EMMETT		54 *
2	0284	PHYSICS DEPARTMENT		54
3	0284	STANFORD UNIVERSITY		54
4	0284	PALO ALTO, CALIF.		54
1	0326	SECRETARY, SPECIAL GROUP ON OPTICAL MASERS	03 COPIES	54
2	0326	ODDRC ADVISORY GROUP ON ELECTRON DEVICES		54
3	0326	346 BROADWAY - 8TH FLOOR		54
4	0326	NEW YORK 13, NEW YORK		54
1	0352	ASD /ASRCE-31/		54
2	0352	WRIGHT-PATTERSON AFB, OHIO		54
1	0354	DR. W. HOLLOWAY		54 *
2	0354	SPERRY RAND RESEARCH CENTER		54
3	0354	SUDBURY, MASSACHUSETTS		54
1	0372	TECHNICAL AREA MANAGER /760B/		54
2	0372	SURVEILLANCE ELECTRONIC SYSTEMS DIVISION		54
3	0372	L. G. HANSCOM AFB		54
4	0372	MASSACHUSETTS		54
5	0372	ATTN MAJOR H. I. JONES, JR.		54
1	0388	COMMANDING OFFICER		54
2	0388	U. S. NAVAL ORDNANCE LABORATORY		54
3	0388	CORONA, CALIF.		54
1	0420	DIRECTOR		54
2	0420	U. S. ARMY ENGINEERING RESEARCH		54
3	0420	AND DEVELOPMENT LABORATORIES		54
4	0420	FORT BELVOIR, VIRGINIA		54
5	0420	ATTN TECHNICAL DOCUMENTS CENTER		54
1	0449	OFFICE OF THE DIRECTOR OF DEFENSE	02 COPIES	54
2	0449	DEFENSE RESEARCH AND ENGINEERING		54
3	0449	INFORMATION OFFICE LIBRARY BRANCH		54
4	0449	PENTAGON BUILDING		54
5	0449	WASHINGTON 25, D. C.		54

1 0471	U. S. ARMY RESEARCH OFFICE	02 COPIES	54
2 0471	BOX CM, DUKE STATION		54
3 0471	DURHAM, NORTH CAROLINA		54
1 0499	DEFENSE DOCUMENTATION CENTER	20 COPIES	54
2 0499	CAMERON STATION BUILDING		54
3 0499	ALEXANDRIA 14, VIRGINIA		54
1 0527	DIRECTOR	06 COPIES	54
2 0527	U. S. NAVAL RESEARCH LABORATORY		54
3 0527	TECHNICAL INFORMATION OFFICER		54
4 0527	CODE 2000, CODE 2021		54
5 0527	WASHINGTON 25, D. C.		54
1 0555	COMMANDING OFFICER		54
2 0555	OFFICE OF NAVAL RESEARCH BRANCH OFFICE		54
3 0555	219 S. DEARBORN ST.		54
4 0555	CHICAGO, ILLINOIS 60604		54
1 0584	COMMANDING OFFICER		54
2 0584	OFFICE OF NAVAL RESEARCH BRANCH OFFICE		54
3 0584	207 W. 24TH ST.		54
4 0584	NEW YORK 11, NEW YORK 10011		54
1 0640	COMMANDING OFFICER		54
2 0640	OFFICE OF NAVAL RESEARCH BRANCH OFFICE		54
3 0640	1000 GEARY STREET		54
4 0640	SAN FRANCISCO, CALIFORNIA 94109		54
1 0696	AIR FORCE OFFICE OF SCIENTIFIC RESEARCH		54
2 0696	WASHINGTON 25, D. C.		54
1 0724	DIRECTOR		54
2 0724	NATIONAL BUREAU OF STANDARDS		54
3 0724	WASHINGTON 25, D. C.		54
1 0752	DIRECTOR		54
2 0752	RESEARCH DEPARTMENT		54
3 0752	U. S. NAVAL ORDNANCE LABORATORY		54
4 0752	WHITE OAK, SILVER SPRING, MD.		54
1 0780	COMMANDING OFFICER		54
2 0780	OFFICE OF NAVAL RESEARCH BRANCH OFFICE		54
3 0780	1030 EAST GREEN STREET		54
4 0780	PASADENA, CALIFORNIA 91101		54
1 0808	COMMANDING OFFICER		54
2 0808	OFFICE OF NAVAL RESEARCH BRANCH OFFICE		54
3 0808	495 SUMMER STREET		54
4 0808	BOSTON 10, MASS.		54

1 0836	U. S. NAVAL RADIOLOGICAL DEFENSE LABORATORY	54
2 0836	/CODE 941/	54
3 0836	SAN FRANCISCO, CALIFORNIA 94135	54
1 0853	COMMANDING OFFICER	54
2 0853	U. S. ARMY MATERIALS RESEARCH AGENCY	54
3 0853	ATTN TECHNICAL LIBRARY	54
4 0853	WATERTOWN, MASSACHUSETTS 02172	54
1 0875	BOULDER LABORATORIES	54
2 0875	NATIONAL BUREAU OF STANDARDS	54
3 0875	ATTN LIBRARY	54
4 0875	BOULDER, COLORADO	54
1 0918	AIR FORCE WEAPONS LABORATORY	54
2 0918	ATTN GUENTHER WLRPF	54
3 0918	KIRTLAND AIR FORCE BASE	54
4 0918	NEW MEXICO	54
1 0932	CHIEF, BUREAU OF NAVAL WEAPONS	54
2 0932	DEPARTMENT OF THE NAVY	54
3 0932	WASHINGTON 25, D. C.	54
4 0932	ATTN J. M. LEE RMGA-81	54
1 0976	AIR FORCE CAMBRIDGE RESEARCH LABORATORIES	54
2 0976	ATTN CRXL-R, RESEARCH LIBRARY	54
3 0976	LAWRENCE G. HANSCOM FIELD	54
4 0976	BEDFORD, MASSACHUSETTS	54
1 0988	BATTELLE MEMORIAL INSTITUTE	54
2 0988	505 KING AVENUE	54
3 0988	COLUMBUS 1, OHIO	54
4 0988	ATTN BMI-DEFENDER	54
1 1030	HEADQUARTERS, USAELRDL	54
2 1030	FORT MONMOUTH, NEW JERSEY 07703	54
3 1030	ATTN SELRA/SAR, NO-4, X, AND PF	54
1 1032	COMMANDER, U. S. NAVAL ORDNANCE TEST STATION	54
2 1032	CHINA LAKE, CALIF	54
3 1032	ATTN MR. G. A. WILKINS /CODE 4041/	54
1 1036	J. C. ALMASI	54 *
2 1036	GENERAL ELECTRIC COMPANY	54
3 1036	ADVANCED TECHNOLOGY LABORATORIES	54
4 1036	SCHENECTADY, N. Y.	54
1 1039	PROF. RUBIN BRAUNSTEIN	54 *
2 1039	UNIVERSITY OF CALIFORNIA	54
3 1039	DEPARTMENT OF PHYSICS	54
4 1039	LOS ANGELES 24, CAL.	54

1	1040	N. I. ADAMS	54 *
2	1040	PERKIN-ELMER CORP.	54
3	1040	NORWALK, CONN.	54
1	1046	E. P. REIDEL	54 *
2	1046	QUANTUM ELECTRONICS DEPT.	54
3	1046	WESTINGHOUSE ELECTRIC CORP.	54
4	1046	RESEARCH LABORATORIES	54
5	1046	PITTSBURGH, PA.	54
1	1047	PROF. H. G. HANSON	54 *
2	1047	UNIVERSITY OF MINNESOTA	54
3	1047	DULUTH, MINN	54
1	1048	P. SCHAFFER	54 *
2	1048	LEXINGTON LABORATORIES, INC.	54
3	1048	84 SHUMAN ST.	54
4	1048	CAMBRIDGE, MASS.	54
1	1049	L. E. RAUTIOILA	54 *
2	1049	LINDE COMPANY, DIVISION OF UNION CARBIDE	54
3	1049	EAST CHICAGO, IND.	54
1	1050	F. S. GALASSO	54 *
2	1050	UNITED AIRCRAFT CORP RESEARCH LABS.	54
3	1050	400 MAIN ST.	54
4	1050	EAST HARTFORD, CONN.	54
1	1051	J. W. NIELSON	54 *
2	1051	AIRTRON, DIVISION OF LITTON INDUSTRIES	54
3	1051	MORRIS PLAINS, N. J.	54
1	1052	E. M. FLANIGEN	54 *
2	1052	LINDE COMPANY	54
3	1052	DIVISION OF UNION CARBIDE	54
4	1052	TONAWANDA, N. Y.	54
1	1053	W. PRINDLE	54 *
2	1053	AMERICAN OPTICAL COMPANY	54
3	1053	14 MECHANIC ST.	54
4	1053	SOUTHBURIDGE, MASS.	54
1	1054	DR. ALAN HAUGHT	54 *
2	1054	PLASMA PHYSICS	54
3	1054	UNITED AIRCRAFT CORP.	54
4	1054	EAST HARTFORD 8, CONN.	54
1	1055	PROF. N. BLOEMBERGEN	54 *
2	1055	HARVARD UNIVERSITY	54
3	1055	DIVISION OF ENGINEERING & APPLIED PHYSICS	54
4	1055	CAMBRIDGE 38, MASS.	54

1	1056	PROF. R. J. COLLINS	54 *
2	1056	UNIVERSITY OF MINNESOTA	54
3	1056	DEPARTMENT OF ELECTRICAL ENG.	54
4	1056	MINNEAPOLIS 14, MINN.	54
1	1057	DR. ALAN KOLB	54 *
2	1057	U. S. NAVAL RESEARCH LAB.	54
3	1057	WASHINGTON, D. C.	54
1	1058	PROF. J. M. FELDMAN	54 *
2	1058	CARNEGIE INSTITUTE OF TECHNOLOGY	54
3	1058	DEPARTMENT OF ELECTRICAL ENGR.	54
4	1058	PITTSBURGH 13, PENNA.	54
1	1059	PROF. ARTHUR SCHAWLOW	54 *
2	1059	STANFORD UNIVERSITY	54
3	1059	STANFORD, CALIFORNIA	54
1	1060	J. ATWOOD	54 *
2	1060	ELECTRO-OPTICAL DIV.	54
3	1060	PERKIN-ELMER CORP.	54
4	1060	NORWALK, CONN.	54
1	1065	RESEARCH MATERIALS INFORMATION CENTER	54
2	1065	OAK RIDGE NATIONAL LABORATORY	54
3	1065	POST OFFICE BOX X	54
4	1065	OAK RIDGE, TENN. 37831	54
5	1065	ATTN MR. T. F. CONNOLLY	54
1	1066	J-5 PLANS AND POLICY DIRECTORATE	54
2	1066	JOINT CHIEFS OF STAFF	54
3	1066	REQUIREMENTS AND DEVELOPMENT DIVISION	54
4	1066	ATTN SPECIAL PROJECTS BRANCH	54
5	1066	ROOM 2D982, THE PENTAGON	54
6	1066	WASHINGTON, D. C., 20301	54
1	1067	ADVANCED RESEARCH PROJECTS AGENCY	54
2	1067	RESEARCH AND DEVELOPEMENT FIELD UNIT	54
3	1067	APO 143, BOX 41	54
4	1067	SAN FRANCISCO, CALIF.	54
1	1068	ADVANCED RESEARCH PROJECTS AGENCY	54
2	1068	RESEARCH & DEVELOPMENT FIELD UNIT	54
3	1068	APO 146, BOX 271	54
4	1068	SAN FRANCISCO, CALIFORNIA	54
5	1068	ATTN MR. TOM BRUNDAGE	54
1	1082	AIR FORCE MATERIALS LABORATORY	54 *
2	1082	AIR FORCE SYSTEMS COMMAND	54
3	1082	WRIGHT-PATTERSON AIR FORCE BASE, OHIO	54
4	1082	ATTN MAAM /LT. JOHN H. ESTESS/	54

1	1083	DR. C. H. CHURCH	54 *
2	1083	WESTINGHOUSE ELECTRIC CORPORATION	54
3	1083	RESEARCH LABORATORIES	54
4	1083	PITTSBURGH 35, PENNA.	54
1	1084	PROF. DONALD S. MCCLURE	54 *
2	1084	INSTITUTE FOR THE STUDY OF METALS	54
3	1084	UNIVERSITY OF CHICAGO	54
4	1084	CHICAGO 37, ILLINOIS	54
1	1085	DR. DANIEL GRAFSTEIN	54 *
2	1085	GENERAL PRECISION, INC.	54
3	1085	AEROSPACE GROUP	54
4	1085	LITTLE FALLS, NEW JERSEY	54
1	1087	DR. R. C. LINARES	54 *
2	1087	PERKIN-ELMER CORPORATION	54
3	1087	SOLID STATE MATERIALS BRANCH	54
4	1087	NORWALK, CONN.	54
1	1088	DR. R. C. OHLMANN	54 *
2	1088	WESTINGHOUSE RESEARCH LABORATORIES	54
3	1088	PITTSBURGH 35, PENNA.	54
1	1089	PROFESSOR S. CLAESSON	54 *
2	1089	UPPSALA UNIVERSITY	54
3	1089	UPPSALA, SWEDEN	54
1	1106	COMMANDING OFFICER	54
2	1106	OFFICE OF NAVAL RESEARCH BRANCH OFFICE	54
3	1106	BOX 39, FPO	54
4	1106	NEW YORK, NEW YORK 09510	54
1	1122	DR. C. U. ELLIS	54 *
2	1122	GPL DIVISION	54
3	1122	GENERAL PRECISION, INC.	54
4	1122	63 BEDFORD ROAD	54
5	1122	PLEASANTVILLE, NEW YORK	54
1	1172	MR. C. M. STICKLEY	54
2	1172	AIR FORCE CAMBRIDGE RESEARCH	54
3	1172	LABORATORIES - CROL	54
4	1172	LAURENCE G. HANSCOM FIELD	54
5	1172	BEDFORD, MASSACHUSETTS 01731	54
1	1177	DR. WAYNE H. KEEN	54 *
2	1177	WESTINGHOUSE DEFENSE & SPACE CENTER	54
3	1177	/SURFACE DIVISION/	54
4	1177	P. O. BOX 1897	54
5	1177	BALTIMORE, MARYLAND 21203	54

1	1178	DR. C. J. KOESTER	54 *
2	1178	AMERICAN OPTICAL COMPANY	54
3	1178	RESEARCH CENTER	54
4	1178	SOUTHBIDGE, MASSACHUSETTS	54
1	1179	DR. RAY HOSKINS	54 *
2	1179	KORAD CORPORATION	54
3	1179	3520 COLORADO AVENUE	54
4	1179	SANTA MONICA, CALIFORNIA 90406	54
1	1180	DR. J. W. CARSON	54 *
2	1180	HUGHES AIRCRAFT COMPANY	54
3	1180	CULVER CITY, CALIFORNIA	54
1	1181	DR. MARVIN LASSER	54 *
2	1181	PHILCO CORPORATION	54
3	1181	RESEARCH LABORATORIES	54
4	1181	BLUE BELL, PENN.	54
1	1183	PROF. A. SMAKULA	54 *
2	1183	CRYSTAL PHYSICS LAB	54
3	1183	MASSACHUSETTS INSTITUTE OF TECHNOLOGY	54
4	1183	CAMBRIDGE, MASS	54
1	1184	DR. F. MCCLUNG	54 *
2	1184	HUGHES RESEARCH LABORATORIES	54
3	1184	3011 MALIBU CANYON ROAD	54
4	1184	MALIBU, CALIFORNIA 90265	54
1	1185	DR. M. C. TOBIN	54 *
2	1185	PERKIN-ELMER CORPORATION	54
3	1185	NORWALK, CONNECTICUT	54
1	1186	PROF. G. W. STROKE	54 *
2	1186	ELECT. ENGINEERING DEPT.	54
3	1186	THE UNIVERSITY OF MICHIGAN	54
4	1186	ANN ARBOR, MICHIGAN 48107	54

FURTHER ADDITIONS TO LIST 54*

Robert L. Parker
National Bureau of Standards
Washington, D. C.

N. D. Schoenberger
Precision Instrument Company
3170 Porter Drive
Palo Alto, California

*Authorized by letter

ONR:421:CES:lm
NR 017-708
30 November 1964

ONR:421 FBI:lsp
13 Nov 1964

FURTHER ADDITIONS TO LIST 54*

Radio Corporation of America
David Sarnoff Research Center
Attn: Dr. R. J. Pressley
Princeton, New Jersey

*Authorized by Distribution List Change Request
NAVEXOS 3703 (4-60)

ONR:421: F. B. Isakson
NR 017-708
2 August 1965